

The four-tank control problem: Comparison of two disturbance rejection control solutions

Original

The four-tank control problem: Comparison of two disturbance rejection control solutions / Huang, Congzhi; Canuto, Enrico; Novara, Carlo. - In: ISA TRANSACTIONS. - ISSN 0019-0578. - 71:(2017), pp. 252-271.
[10.1016/j.isatra.2017.07.020]

Availability:

This version is available at: 11583/2678904 since: 2018-02-27T18:44:26Z

Publisher:

ISA - Instrumentation, Systems, and Automation Society

Published

DOI:10.1016/j.isatra.2017.07.020

Terms of use:

This article is made available under terms and conditions as specified in the corresponding bibliographic description in the repository

Publisher copyright

(Article begins on next page)

The four-tank control problem: comparison of two disturbance rejection control solutions

Congzhi Huang¹, Enrico Canuto²

¹ School of Control and Computer Engineering, North China Electric Power University, Beijing, 102206, China

E-mail: hcz190@ncepu.edu.cn

² Politecnico di Torino, Dipartimento di Automatica e Informatica, Corso Duca degli Abruzzi 24, 10129 Torino, Italy

Email: enrico.canuto@polito.it

Abstract

The paper aims to compare and prove a pair of disturbance/uncertainty rejection control laws for the well-known four tank control problems. Control requirements are expressed in terms of a set point sequence as it usual in the literature. Uncertainty class is defined as the union of four sub-classes: unknown disturbance, parametric uncertainty, measurement errors and neglected dynamics. Modelling and design allow insight of the dynamic properties of the problem. They are formulated by a pair of theorems which fix the range of application. Theorems are confirmed by the results of simulated runs, and indicate the correct way to further broaden control design applicability. Disturbance rejection (better uncertainty) design is deployed using the Embedded Model Control methodology: only unknown disturbance and parametric uncertainty can be rejected, whereas neglected dynamics effects must be filtered. As a result, simple performance and stability inequality can be formulated in the frequency domain and lead to closed-loop pole placement. Inequalities are such to reveal whether pole placement is feasible and how feasibility can be recovered, an issue which at authors knowledge is rarely encountered in the literature. Simulated runs prove the design procedure.

Index Terms: four-tank benchmark, embedded model control, state predictor, disturbance rejection

1. Introduction

The classical four-tank benchmark, initially proposed by Johansson in [1] and [2] is a test platform for comparing control strategies. The benchmark is a representation of multivariable control instances: the mathematical model of the process is nonlinear, the process is highly coupled, the four tank levels are available in real time with the aid of sensors installed on the equipment, dynamic properties (say minimum and non-

minimum phase) and relevant control performance change by varying the pump flow distribution and consequently the four-tank interaction degree. The problem has been investigated by several scholars in the past decades, and experimental tests have been made on laboratory-scale equipment [3]. Since the four-tank experiment is suited to demonstrate multivariable control concepts, it has been introduced in several university laboratories [4].

To deal with coupling and nonlinearity, various control approaches have been applied and their performance compared [5]. Two kinds of decentralized PI controllers were designed and validated in [6]. PID controllers were designed for a modified quadruple-tank process by using inverted decoupling and root locus technique [7]. To deal with minimum and non-minimum phase behavior, improvement of PID controllers was investigated in [8].

Model-based predictive control algorithms were designed and implemented within the European project HD-MPC [9]. Five different decentralized control strategies based on a distributed multi-parametric model predictive control were proposed in [10]. A model predictive controller based on a linearized state-space model was designed and tested in [11]. A fast gradient-based distributed optimization approach was applied to a hierarchical and distributed model predictive control in [12]. Nonlinear generalized predictive control and back-stepping approach were applied and tested in [13].

Besides the model predictive control, nonlinear control approach was also employed. A two-level control algorithm was developed in [14] for the robust optimal control of large-scale nonlinear systems with unstructured bounded uncertainties. Taking the four-tank process as case study, nonlinear approach and dynamic optimization were validated in [15].

Feedback linearization and sliding mode control were proposed and tested in [16]. Sliding model control was adopted to cope with parametric uncertainty. A fractional-order sliding mode controller was designed and tested in [17]. A fuzzy modified model reference adaptive control approach was proposed in [18]. To deal with the multivariable dead times, decentralized integral controllability and time-domain bounds on closed loop performance were derived and discussed, and a laboratory process was described and tested in [19]. Other studies refer to simulation [20] and fault-diagnosis [21]. Most of the approaches focused on continuous-time control design. An optimal discrete-time (DT) linear controller was proposed and tested in [22].

Most of the above studies assume the presence of unknown but bounded input signals, but none of them extends the design model to include disturbance dynamics, in order to estimate and reject unknown disturbance and parametric uncertainty. In fact, the main goal is to just design robust feedback control laws, without any intermediate state observer. A different approach has been proposed and tested by simulated runs in [23]. Firstly, feedback linearization is performed by taking the derivatives of two ‘flat’ variables as they lead to a multivariate normal form of process equations. Then, input nonlinear terms and stochastic disturbances are together estimated and actively rejected, in agreement with the Active Disturbance Rejection Control (ADRC) and extended

state observers (ESO) [24].

This paper follows the way opened by [23], but the uncertainty domain is extended to include neglected dynamics and parametric uncertainty. As a second extension, control algorithms are directly designed in the discrete-time domain on the basis of the so called embedded model, which is a kind of internal model at the core of the control unit. According to the Embedded Model Control (EMC, [25], [26]) methodology, embedded model must include suitable disturbance dynamics (not necessarily first order as in ESO and ADRC), which is driven by arbitrary bounded signals playing the role of driving noise. Model endowment with disturbance dynamics is a key tool for decoupling control strategies as shown in [27] and [28]. As a third extension, the disturbance observer feedback is allowed to be a dynamic system when a static feedback cannot guarantee closed-loop stability [28], [29]. In fact, the state observer feedback is conceived as an output to noise (not as an output to state) feedback, which implies that when driving noise is singular, i.e. noise dimensionality is lower than model state, missing feedback channels must be recovered through dynamic feedback. To better understand the issue, think of the Kalman filter feedback when input noise is singular (i.e. input covariance is singular). Since the filter feedback is static, closed-loop stability demands all the state variables, also the noise-free ones, to be excited by a feedback component. EMC follows a different way: noise layout must be designed as in [30] and [31] according to the desired uncertainty class; embedded model should not be corrupted by parasitic noise. Since noise plays the role of the uncertainty input, this way offers flexibility and efficiency in the real-time uncertainty estimation and discrimination. As a fourth extension, a gain tuning procedure is available which exploits the relation between pole placement and asymptotic closed-loop transfer functions [32]. EMC has been applied to space and industrial control systems [33], [34].

The paper goal is to understand and enlighten, through EMC design, the four-tank decoupled control performance and limitations in the presence of all kinds of uncertainty. Analysis and design exploits uncertainty/disturbance estimation and rejection. To this end, we proceed in two steps. First, a simple decoupled control is proposed, based on a first-order feedback linearization which is affected by zero dynamics (problem A). The decoupled control is shown to achieve perfect tracking, under ideal disturbance rejection, only when zero dynamics is stable, which is a reasonable condition in practice. As a second step, in order to achieve perfect tracking also under non minimum phase conditions, a feedback linearization as proposed in [23] is adopted since it is free of zero dynamics (problem B). It will be shown that the corresponding decoupled control is capable of achieving perfect tracking only in absence of unknown disturbances. This would suggest a third step which adopted a feedback linearization and a decoupled control capable of ensuring perfect tracking under any phase condition and uncertainty domain. Although this step is not pursued here for brevity's sake, solutions of the paper may be of interest both theoretically and practically; moreover, by revealing difficulties pave the way to a complete solution.

The paper is organized in the following way. In Section 2, firstly, the four-tank state

equations are recalled, the uncertainty class and the performance variables of the problems A and B are defined. A unifying formulation of the two control problems is given and the reachable set of constant references (set points) is derived. Feedback linearization is performed for each problem and the relevant ideal control laws are derived. Limitations of the ideal laws are expressed by two theorems. Section 3 is devoted to the EMC implementation of the ideal control laws derived in Section 2, by means of embedded model, noise estimator, reference generator and control law. Section 3 ends by showing how to tune the different gains of the EMC control algorithms in order to achieve the requested tracking accuracy. Section 4 provides the data and the uncertainty domain of the simulated environment, and the simulated results of each control design (A and B). Discussion and comparison of the results is provided.

2. Model, uncertainty and control problems

2.1. State equations

The schematic diagram of the four-tank benchmark is in Fig.1 [9].

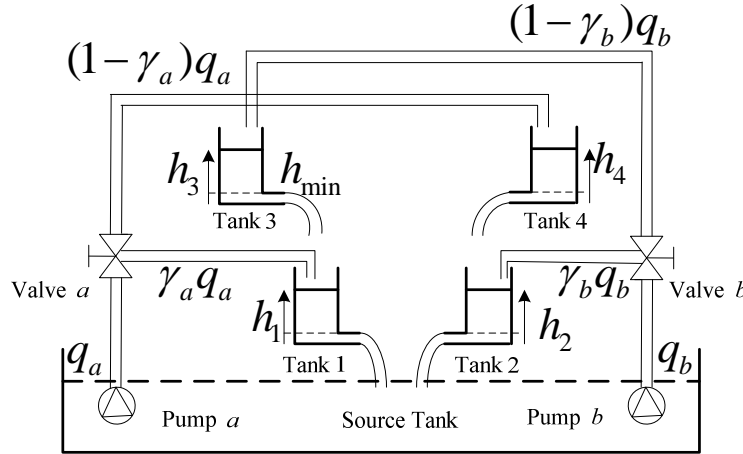


Fig. 1. Schematic diagram of the four-tank benchmark process.

The four tanks $k = 1, 2, 3, 4$ in Fig.1 are fed by liquid pumped from the storage tank, and the liquid level h_k of each tank, in meter, is measured by a pressure sensor. The sensor measurement becomes unreliable as soon as the level approaches zero. To prevent this, the tank level is only controlled above a common minimum level h_{min} . The state variable $x_k = h_k - h_{min}$ is the controlled liquid level of the k -th tank. The measurement of the controlled level x_k level is indicated by y_k . The maximum level is denoted by $h_{k,max}$ as it may vary from tank to tank. The cross section area of each tank is S_k . The discharge constant of the k -th tank, in square meter, is denoted by a_k . The volume flows q_a and q_b , in cubic meter per second, which are supplied by pumps a and b , are the process commands. Aperture fraction coefficients of the three-way flow valves are denoted by γ_a and γ_b , respectively.

Tanks 1 and 3 are supplied by pump a through the valve a with fractions γ_a and $1 - \gamma_a$, respectively. Both fractions are collected in the vector γ . Liquid pumped from

the pump b supplies tank 2 with a fraction of γ_b , the remaining fraction $1 - \gamma_b$ supplies tank 4. Liquid in tanks 3 and 1 discharges by gravity into tank 1 and the storage tank, respectively. Discharge is permitted by bottom orifices having discharge constants a_3 and a_1 . In parallel, liquid in tanks 4 and 2 drains by gravity into tank 2 and the storage tank. Their bottom orifices have discharge constants a_4 and a_2 . The admissible set of the valve fraction coefficients is $\Gamma = \{\Gamma_a, \Gamma_b\}$, with $\Gamma_a = \{0 \leq \gamma_a \leq 1\}$ and $\Gamma_b = \{0 \leq \gamma_b \leq 1\}$. By adjusting $\gamma \in \Gamma$, the process dynamics may significantly vary. Each tank is subject to disturbance flows which can be interpreted as the uncertainty of the pump supply flows and of the discharge flows, and also as leakages or external withdrawals.

Performance variables are related to a pair of control problems to be treated in this paper.

Problem A: lower tank level regulation. The goal is to regulate the level $z_k = x_k$, $k = 1, 2$ of the lower tanks 1 and 2 around some set point, by acting on the pump flows q_a and q_b . The level x_k , $k = 3, 4$ of the upper tanks is left unregulated. The set of the performance variables is denoted by $Z = \{z_1, z_2\}$. ■

Problem B: four-tank level regulation. The goal is to regulate the level of the four tanks by directly regulating a pair of combinations $R = \{r_1, r_2\}$ of the tank levels, namely

$$\begin{aligned} r_1 &= (1 - \gamma_a)x_1 - \gamma_a x_4 \\ r_2 &= (1 - \gamma_b)x_2 - \gamma_b x_3 \end{aligned} \quad (1)$$

In problem B, Γ is restricted to $\gamma_a < 1$ and $\gamma_b < 1$ for avoiding lower tanks to be excluded. ■

Problem A will be addressed by assuming that the discharge flows from tank 3 to 1 and from tank 4 to 2 are just disturbances to be compensated. It will be proved that in subset $\Gamma_0 \subset \Gamma$ of the valve fractions this compensation cannot be achieved, which demands that also upper tanks be regulated in their level. A remedy suggested by [23] is to regulate the combination (1) of the four tank levels (Problem B), which control should entrain regulation of the bottom tank level. It will be shown that the objective can only be achieved in absence of unknown disturbances.

The affine state equations, which are obtained from mass balance and Bernoulli's law, read as follows:

$$\begin{aligned} \dot{x}(t) &= Ap(x(t)) + Bq(t - \tau_u) + q_d(t), x(0) = x_0 \\ y(t) &= Cx(t - \tau_y) + e_y(t) \\ z(t) &= \begin{bmatrix} z_{12} \\ r_{12} \end{bmatrix} = \begin{bmatrix} F_z \\ F_r \end{bmatrix} x(t) = Fx(t) \end{aligned} \quad , \quad (2)$$

where $0 \leq x(t) \leq x_{max}$ represents the state vector (m), p is the tank discharge rate (m/s), $0 \leq q(t) \leq q_{max}$ is the flow command (m³/s), q_d is an unknown level rate disturbance (m/s), y is the measurement vector (m), e_y is the measurement error, and z is the overall performance vector to be controlled by Problems A and B. Components

of x_{max} are denoted with $x_{k,max}$, $k = 1, \dots, 4$, and those of q_{max} with $q_{j,max}$, $j = a, b$. Components of p have the expression $p_k = S_k^{-1} a_k \sqrt{2g x_k} = P_k \sqrt{x_k}$. For later use the vector \sqrt{x} with components $\sqrt{x_k}$ is defined. State and command vectors are bounded. Actuator and sensor delays are denoted by τ_u and τ_y , respectively. State, command and output vectors in (2) are given below:

$$\begin{aligned} x = \begin{bmatrix} x_1 \\ x_2 \\ x_3 \\ x_4 \end{bmatrix} = \begin{bmatrix} x_{12} \\ x_{34} \end{bmatrix}, p(x) = \begin{bmatrix} p_1(x_1) \\ p_2(x_2) \\ p_3(x_3) \\ p_4(x_4) \end{bmatrix}, q = \begin{bmatrix} q_a \\ q_b \end{bmatrix}, q_d = \begin{bmatrix} q_{d1} \\ q_{d2} \\ q_{d3} \\ q_{d4} \end{bmatrix} \\ y = \begin{bmatrix} y_1 \\ y_2 \\ y_3 \\ y_4 \end{bmatrix}, e_y = \begin{bmatrix} e_{y1} \\ e_{y2} \\ e_{y3} \\ e_{y4} \end{bmatrix}, z = \begin{bmatrix} z_{12} \\ r_{12} \end{bmatrix} = \begin{bmatrix} z_1 \\ z_2 \\ r_1 \\ r_2 \end{bmatrix} \end{aligned} \quad (3)$$

State, command and output matrices in (2) have the following components

$$\begin{aligned} A = \begin{bmatrix} -1 & 0 & 1 & 0 \\ 0 & -1 & 0 & 1 \\ 0 & 0 & -1 & 0 \\ 0 & 0 & 0 & -1 \end{bmatrix} = \begin{bmatrix} -I_2 & I_2 \\ 0 & -I_2 \end{bmatrix} \\ B = \begin{bmatrix} \frac{\gamma_a}{s_1} & 0 \\ 0 & \frac{\gamma_b}{s_2} \\ 0 & \frac{1-\gamma_b}{s_3} \\ \frac{1-\gamma_a}{s_4} & 0 \end{bmatrix} = \begin{bmatrix} B_{12} \\ B_{34} \end{bmatrix}, C = \begin{bmatrix} c_1 & 0 & 1 & 0 \\ 0 & c_2 & 0 & 1 \\ 0 & 0 & c_3 & 0 \\ 0 & 0 & 0 & c_4 \end{bmatrix} \\ F_z = \begin{bmatrix} 1 & 0 & 0 & 0 \\ 0 & 1 & 0 & 0 \end{bmatrix}, F_r = \begin{bmatrix} 1-\gamma_a & 0 & 0 & -\gamma_a \\ 0 & 1-\gamma_b & -\gamma_b & 0 \end{bmatrix} = [F_{r1} \quad F_{r2}] \end{aligned} \quad (4)$$

All parameters in (2) are uncertain but bounded. Given a generic parameter π_j , $j = 1, j = 1, 2, \dots, N_\pi$, uncertainty is written as follows:

$$\pi_j = \pi_{j,nom}(1 + \pi_j), |\delta\pi_j| \ll 1.$$

where $\pi_{j,nom}$ is the nominal value which is known to control designer, and $\delta\pi_j$ denotes bounded fractional uncertainty. Let us denote the parametric uncertainty bounded set by Π . The parameters $c_k = 1 + \epsilon_k$, $k = 1, \dots, 4$ in C account for the scale factor error ϵ_k . Actuator and sensor delays are assumed to be unknown and bounded, namely $\tau_u \leq \tau_{u,max}$, $\tau_y \leq \tau_{y,max}$. Such bounds define the uncertainty class **E** of neglected dynamics to be made explicitly in Section 3. The class may be shrunk by assuming that delays are partly known.

The third uncertainty set is the class **D** of the unknown disturbance q_d . Each component q_{dk} is assumed to be approximated by discrete-time arbitrary piecewise linear signals driven by bounded zero-mean arbitrary signals (briefly ‘noise’). In other terms, given a time unit T , $q_{dk}(t_i = iT)$ is formulated by the following linear and time-invariant (LTI) state equation

$$\begin{aligned} \begin{bmatrix} x_{dk} \\ x_{sk} \end{bmatrix} (i+1) &= \begin{bmatrix} 1 & 1 \\ 0 & 1 \end{bmatrix} \begin{bmatrix} x_{dk} \\ x_{sk} \end{bmatrix} (i) + \begin{bmatrix} w_{dk} \\ w_{sk} \end{bmatrix} (i), \begin{bmatrix} x_{dk} \\ x_{sk} \end{bmatrix} (0) = \begin{bmatrix} x_{dk,0} \\ x_{sk,0} \end{bmatrix}, \\ q_{dk}(i) &= [1 \quad 0] \begin{bmatrix} x_{dk} \\ x_{sk} \end{bmatrix} (i) + w_{xk}(i) \end{aligned} \quad (5)$$

where the noise bound is $|w_{jk}(i)| \leq w_{jk,max}, j = d, s, x$ and zero mean is defined by $\lim_{N \rightarrow \infty} \frac{1}{N} \sum_{i=0}^{N-1} w_{jk}(i) = 0$.

The forced response of q_{dk} in (5) is an unbounded arbitrary piecewise linear signal corrupted by noise w_{qk} . Equation (5) can be converted into a stochastic equation by assuming that $w_{jk}(i), j = d, s, x$ is a zero-mean white noise with bounded variance. Noise components are assumed to be uncorrelated. In this case q_{dk} is a second order random drift corrupted by noise. In both cases \mathbf{D} is a class of unbounded signals, which cannot be rejected by bounded commands. However, q_{dk} can be given a bound by shifting the unit eigenvalues of (5) inside the unit circle, but changing equation (5) to become parameter dependent. We will adopt a trade-off: (i) the parameter-free equation (5) will be part of the embedded model, since parameter freedom is favouring stability robustness; (ii) signals of \mathbf{D} will be assumed to have a known bound when control gains are tuned for guaranteeing performance. In practice, if a bound overshoot occurs, performance will degrade, a subject not treated here.

The last set \mathbf{W}_y is the set of the DT measurement errors $e_y(t_i)$, which includes output quantization errors, and may be modelled as a bounded variance zero-mean white noise.

The relation with the DT control unit command $q(i)$ is given by

$$\begin{aligned} q(t) &= R_u \text{int}(R_u^{-1} q(i)), \begin{bmatrix} 0 \\ 0 \end{bmatrix} \leq \text{int}(R_u^{-1} q(i)) < \begin{bmatrix} N_u \\ N_u \end{bmatrix} \\ R_u &= \begin{bmatrix} \rho_a & 0 \\ 0 & \rho_b \end{bmatrix}, \rho_j \frac{q_{j,max}}{N_u}, j = a, b \end{aligned} \quad (6)$$

where ρ_j is the quantization level of the flow command q_j and i denotes the DT instant $t_i = iT$. T is the control time unit. A similar conversion defines the measurement vector $y(i)$ which is employed by the control unit:

$$\begin{aligned} y(i) &= R_y \text{int}(R_y^{-1} y(t_i)), \begin{bmatrix} 0 \\ 0 \\ 0 \\ 0 \end{bmatrix} \leq \text{int}(R_y^{-1} y(i)) < \begin{bmatrix} N_y \\ N_y \\ N_y \\ N_y \end{bmatrix} \\ R_y &= \begin{bmatrix} \rho_1 & 0 & 0 & 0 \\ 0 & \rho_2 & 0 & 0 \\ 0 & 0 & \rho_3 & 0 \\ 0 & 0 & 0 & \rho_4 \end{bmatrix}, \rho_k = \frac{x_{k,max}}{N_y}, k = 1, 2, 3, 4 \end{aligned} \quad (7)$$

Eq.(6) and Eq. (7) are responsible for command and measurement quantization errors. Command errors are accounted for by the unknown disturbance q_d in (2), measurement errors by the error e in (2).

For later use Ap in (2) can be rewritten as

$$Ap = AP\sqrt{x} \\ P = \begin{bmatrix} P_1 & 0 & 0 & 0 \\ 0 & P_2 & 0 & 0 \\ 0 & 0 & P_3 & 0 \\ 0 & 0 & 0 & P_4 \end{bmatrix} = \begin{bmatrix} P_{12} & 0 \\ 0 & P_{34} \end{bmatrix}, \sqrt{x} = \begin{bmatrix} \sqrt{x_1} \\ \sqrt{x_2} \\ \sqrt{x_3} \\ \sqrt{x_4} \end{bmatrix} = \begin{bmatrix} \sqrt{x_{12}} \\ \sqrt{x_{34}} \end{bmatrix}. \quad (8)$$

2.2. Control problem formulation and admissible set

Both control problems A and B can be formulated as follows.

Control problem formulation. Given a discrete time $t_i = iT$, T being the time unit, and a set \mathbf{Z}_{ref} of piecewise constant reference trajectories $z_{ref}(t)$ for the sampled performance vector $z(t)$ in (2), we demand that the ‘true’ tracking error $e_{ref}(t) = z_{ref}(t) - z(t)$ is bounded and the sampled mean value tends to zero as follows

$$\begin{aligned} |e_{k,ref}(t)| &\leq e_{k,max}, t_j + \tau_s \leq t < t_{j+1} \\ \lim_{N \rightarrow \infty} \frac{1}{N} \prod_{i=0}^{N-1} e_{k,ref}(t_i) &= 0 \end{aligned} \quad (9)$$

In (9), $e_{k,ref}$ is a component of e_{ref} , t_j is a jump time of the reference trajectories and τ_s is a feasible settling time interval imposed by control requirements. The above inequality and asymptotic equality must hold within the uncertainty class previously defined. We assume that the derivative $\dot{z}_{ref}(t)$ is bounded, i.e. there is continuity between two successive constant values (set points) of $z_{ref}(t)$. ■

Any component $z_{k,ref}(t)$ of z_{ref} must be feasible, i.e. $z_{k,ref}(t)$ at any t must be a reachable equilibrium point. Using (8), the equilibrium equation under $q_d = 0$ in (2) becomes

$$AP\sqrt{x} = B(\gamma)q. \quad (10)$$

Given a command vector q , the equation has a unique solution since AP is invertible. Exploiting the upper triangular form of A , the square root $\sqrt{x_{12}}$ of the lower tank levels and the root $\sqrt{x_{34}}$ of the upper tank levels can be solved separately as

$$\begin{aligned} \sqrt{x_{12}} &= P_{12}^{-1} \Delta B(\gamma)q \\ \sqrt{x_{34}} &= P_{34}^{-1} B_{34}(\gamma)q \\ \Delta B(\gamma) &= B_{12}(\gamma) + B_{34}(\gamma) = \begin{bmatrix} \frac{\gamma_a}{s_1} & \frac{1-\gamma_b}{s_3} \\ \frac{1-\gamma_a}{s_4} & \frac{\gamma_b}{s_2} \end{bmatrix}. \end{aligned} \quad (11)$$

The solution of equation (10) must also satisfy bounds on x and q in order to define admissible reference trajectories. We give the following definition.

Definition 1. Given the fraction vector γ , an equilibrium pair (x_{eq}, q_{eq}) satisfying (10) is said to be admissible, i.e. belonging to $\mathbf{A}(\gamma)$, if and only if it satisfies command and level bounds:

$$0 \leq q_{eq} \leq q_{max}, \quad 0 \leq x_{eq} \leq x_{max}. \quad (12)$$

For the problem A which aims to regulate lower tank levels, the interest is in finding an expression of $\mathbf{A}(\gamma)$ in terms of x_{12} . This is feasible since equation (10) has a

unique solution also given either $\sqrt{x_{12}}$ or $\sqrt{x_{34}}$. The expression is obtained by inverting equation (11) in order to obtain $q(x_{12})$ and $x_{34}(x_{12})$. We proceed in two steps. The bounds on $q(x_{12})$ and x_{12} define the admissible set $\mathbf{A}_q(\gamma)$. The bounds on $x_{34}(x_{12})$ define $\mathbf{A}_{34}(\gamma)$. Then $\mathbf{A}(\gamma) = \mathbf{A}_q(\gamma) \cap \mathbf{A}_{34}(\gamma)$. $\mathbf{A}_q(\gamma)$ is expressed by

$$0 \leq q_{min} \leq q(x_{12}) = \Delta B^{-1}(\gamma) P_{12} \sqrt{x_{12}} \leq q_{max} \leq \sqrt{x_{12,max}}$$

$$\Delta B^{-1}(\gamma) P_{12} = \frac{S_3 S_4 \sqrt{2g}}{\gamma_a \gamma_b \left(\frac{S_3 S_4}{S_1 S_2} - 1 \right) + \gamma_a + \gamma_b - 1} \begin{bmatrix} \frac{a_1 \gamma_b}{S_1 S_2} & -a_2 \frac{1-\gamma_b}{S_2 S_3} \\ -a_1 \frac{1-\gamma_a}{S_1 S_4} & \frac{a_2 \gamma_a}{S_1 S_2} \end{bmatrix}. \quad (13)$$

The admissible set $\mathbf{A}_{34}(\gamma)$ expression is found to be

$$0 \leq \sqrt{x_{34}(x_{12})} = P_{34}^{-1} B_{34}(\gamma) \Delta B^{-1}(\gamma) P_{12} \sqrt{x_{12}} \leq \sqrt{x_{34,max}}$$

$$P_{34}^{-1} B_{34}(\gamma) = \frac{1}{\sqrt{2g}} \begin{bmatrix} 0 & -\frac{1-\gamma_b}{a_3} \\ -\frac{1-\gamma_a}{a_4} & 0 \end{bmatrix} \quad (14)$$

The admissible region of $\mathbf{A}(\gamma)$ in the positive quadrant of x_{12} is a parallelogram having a vertex in the origin. The parallelogram may be truncated by the level bound $x_{12,max}$. The set shrinks to a line when $\Delta B(\gamma)$ becomes singular which occurs for

$$\beta(\gamma) = \gamma_a \gamma_b \left(\frac{S_3 S_4}{S_1 S_2} - 1 \right) + \gamma_a + \gamma_b - 1 = 0. \quad (15)$$

The ‘critical coefficient’ $\beta(\gamma)$ will play a fundamental role in control design and performance.

In the uniform case defined by $S_k = S$ and $a_k = a$, $\mathbf{A}_q(\gamma)$ simplifies to

$$0 \leq \begin{bmatrix} q_{a,min} \\ q_{b,min} \end{bmatrix} \leq \frac{\sqrt{2g}}{\gamma_a + \gamma_b - 1} \begin{bmatrix} \gamma_b & -(1-\gamma_b) \\ -(1-\gamma_a) & \gamma_a \end{bmatrix} \begin{bmatrix} \sqrt{x_1} \\ \sqrt{x_2} \end{bmatrix} \leq \begin{bmatrix} q_{a,max} \\ q_{b,max} \end{bmatrix}, \quad (16)$$

and in the singular case $\gamma_a + \gamma_b = 1$, to the segment of the line $a_1(1-\gamma_a)\sqrt{x_1} + a_2\gamma_a\sqrt{x_2} = 0$. $\mathbf{A}_{34}(\gamma)$ simplifies to

$$0 \leq \frac{1}{\gamma_a + \gamma_b - 1} \begin{bmatrix} -(1-\gamma_a)(1-\gamma_b) & (1-\gamma_b)\gamma_a \\ (1-\gamma_a)\gamma_b & -(1-\gamma_a)(1-\gamma_b) \end{bmatrix} \begin{bmatrix} \sqrt{x_1} \\ \sqrt{x_2} \end{bmatrix} \leq \begin{bmatrix} \sqrt{x_{3,max}} \\ \sqrt{x_{4,max}} \end{bmatrix}. \quad (17)$$

Fig. 2 shows the Monte Carlo regions of two typical admissible sets $\mathbf{A}(\gamma)$ (blue dots) under different values of the critical coefficient $\beta(\gamma)$, in the not uniform case and for $q_{min} = 0$. On Fig. 2, left, we have $\beta(\gamma) > 0$ and $\mathbf{A}(\gamma) = \mathbf{A}_q(\gamma) = \mathbf{A}_{34}(\gamma)$. The parallelogram is truncated on the right side and the top by the lower tank bounds. On Fig. 2, right, we have $\beta(\gamma) < 0$ and $\mathbf{A}(\gamma) = \mathbf{A}_{34}(\gamma)$ (blue dots) is such to narrow $\mathbf{A}_q(\gamma)$ (black dots). This confirms that $\beta(\gamma) > 0$ is in favour of lower tank regulation. Both admissible regions in Fig. 2 shrink to a line for $\beta(\gamma) \rightarrow 0$ and to a rectangle for $\beta(\gamma) \rightarrow (S_1 S_2)^{-1} S_3 S_4$ (Fig. 2, left) and for $\beta(\gamma) \rightarrow -1$ (Fig. 2, right).

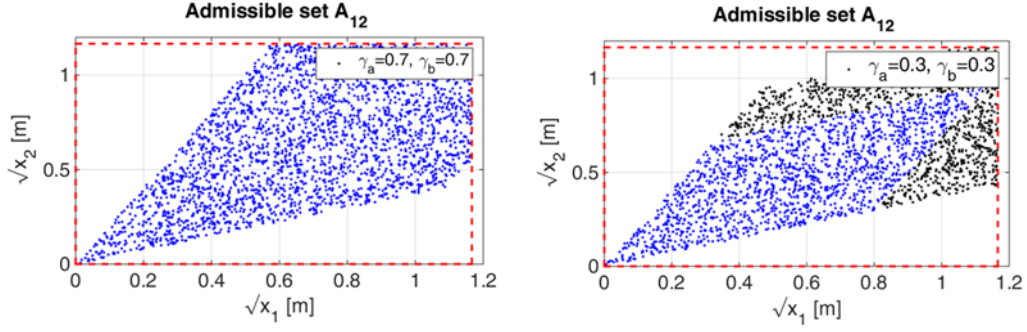


Fig. 2. The admissible set $\mathbf{A}(\gamma)$ under different critical coefficient values: left, $\beta(\gamma) > 0$, right, $\beta(\gamma) < 0$.

Fig. 3 shows the admissible set $\mathbf{A}(\gamma)$ close to a line for $\beta(\gamma) = 0.01$ and in the not uniform case.

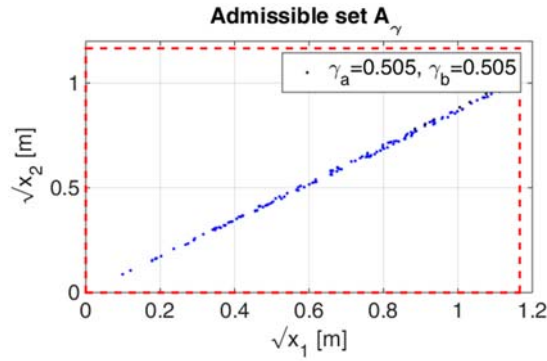


Fig. 3. Admissible set for $\beta(\gamma) \cong 0$.

As a conclusion the reference set \mathbf{Z}_{ref} strictly depends on the selected valve fraction γ and must hold $\mathbf{Z}_{ref} \subseteq \mathbf{A}(\gamma)$. The reference generator to be mentioned in Section 3 is in charge of recovering $\mathbf{Z}_{ref} \subseteq \mathbf{A}(\gamma)$ either by adapting γ or \mathbf{Z}_{ref} . The admissible set must account also for disturbance rejection, which is such to shrink the command range. To this end, q_{min} in equation (13) must be found on the basis of the disturbance class.

Assume now that, for reasons to become clear in Section 2.3, either or both upper tank levels reach saturation. In this case, assuming for simplicity's sake the uniform case $S_k = S$, $a_k = a$ and $x_{k,max} = x_{max}$, either or both components of (16) and (17) are replaced by the set \mathbf{A}_{sat} defined by

$$\begin{aligned} 0 \leq \gamma_a q_{a,min} \leq \sqrt{2g}(\sqrt{x_1} - \sqrt{x_{max}}) \leq \gamma_a q_{a,max}, 0 \leq x_1 \leq x_{max} \\ 0 \leq \gamma_b q_{b,min} \leq \sqrt{2g}(\sqrt{x_2} - \sqrt{x_{max}}) \leq \gamma_b q_{b,max}, 0 \leq x_2 \leq x_{max} \end{aligned} \quad (18)$$

The set \mathbf{A}_{sat} is always empty. The set may include a small rectangular region of the positive quadrant of x_{12} only in the not uniform case. The reason is that the discharge from upper to lower tanks may become excessive, thus demanding negative command, which is assumed not admissible in (2). Fig. 4 compares $\mathbf{A}(\gamma)$ with $\gamma_a = \gamma_b = 0.7$ to \mathbf{A}_{sat} in the not uniform case. In the uniform case the latter one would be empty.

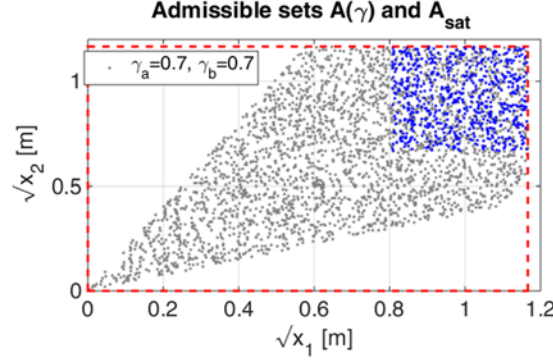


Fig. 4. Admissible set without (grey dots) and with upper tank saturation (blue dots).

2.3. Problem A: ideal control law and zero dynamics

Consider Problem A and assume non zero disturbance q_d . Assume that a constant reference $z_{k,ref}, k = 1, 2$ is exactly tracked, i.e. $\dot{x}_k = 0, k = 1, 2$, which implies that the following control law equality holds

$$\begin{bmatrix} q_a \\ q_b \end{bmatrix}(t) = \begin{bmatrix} \frac{S_1}{\gamma_a} (p_1 - p_3 - q_{d1}) \\ \frac{S_2}{\gamma_b} (p_2 - p_4 - q_{d2}) \end{bmatrix}(t). \quad (19)$$

Equation (17) corresponds to the first equation in (11) if we assume $q_d = 0$ and constant level of the upper tanks. Here the interest is to investigate the interaction of the lower tank regulation with unregulated upper tanks.

By replacing (17) in (2), state equations in the feedback linearization normal form are obtained

$$\begin{aligned} \begin{bmatrix} \dot{x}_1 \\ \dot{x}_2 \end{bmatrix}(t) &= 0, \begin{bmatrix} x_1 \\ x_2 \end{bmatrix}(0) = \begin{bmatrix} x_{10} \\ x_{20} \end{bmatrix} \\ \begin{bmatrix} \dot{x}_3 \\ \dot{x}_4 \end{bmatrix}(t) &= \begin{bmatrix} -p_3 + \frac{S_2}{S_3} \frac{1-\gamma_b}{\gamma_b} (p_2 - p_4) \\ -p_4 + \frac{S_1}{S_4} \frac{1-\gamma_a}{\gamma_a} (p_1 - p_3) \end{bmatrix} + \begin{bmatrix} q_{d3} - \frac{S_2}{S_3} \frac{1-\gamma_b}{\gamma_b} q_{d2} \\ q_{d4} - \frac{S_1}{S_4} \frac{1-\gamma_a}{\gamma_a} q_{d1} \end{bmatrix}, \begin{bmatrix} x_3 \\ x_4 \end{bmatrix}(0) = \begin{bmatrix} x_{30} \\ x_{40} \end{bmatrix}. \end{aligned} \quad (20)$$

The first equation is linear and time invariant (LTI) and can be stabilized by adding to (17) the state feedback command

$$\begin{bmatrix} \Delta q_a \\ \Delta q_b \end{bmatrix}(t) = \begin{bmatrix} \frac{S_1 K_1}{\gamma_a} & 0 \\ 0 & \frac{S_2 K_2}{\gamma_b} \end{bmatrix} \begin{bmatrix} z_{1,ref} - x_1 \\ z_{2,ref} - x_2 \end{bmatrix}(t), K_1 > 0, K_2 > 0. \quad (21)$$

The second equation is the zero dynamics of the Problem A. In other terms, under (17) state equation (2) exhibits relative degree one with respect to q

Observe that the total control law made by (17) and (19) cannot be realized because the state variables must be replaced by measurements and the unknown disturbance must be estimated.

Properties of zero dynamics are studied as in [23] through the state and command perturbations $\delta x = x - x_{eq}$ and $\delta q = q - q_{eq}$ of an equilibrium pair (x_{eq}, q_{eq}) defined in (12) under $q_d = 0$. The corresponding linear perturbation equation of (18) and (19) holds

$$\begin{aligned}
 \begin{bmatrix} \delta \dot{x}_1 \\ \delta \dot{x}_2 \end{bmatrix} (t) &= - \begin{bmatrix} K_1 & 0 \\ 0 & K_2 \end{bmatrix} \begin{bmatrix} \delta x_1 \\ \delta x_2 \end{bmatrix} (t), \begin{bmatrix} \delta x_1 \\ \delta x_2 \end{bmatrix} (0) = \begin{bmatrix} \delta x_{10} \\ \delta x_{20} \end{bmatrix} \\
 \begin{bmatrix} \delta \dot{x}_3 \\ \delta \dot{x}_4 \end{bmatrix} (t) &= - \begin{bmatrix} \frac{P_3}{2\sqrt{x_{3,eq}}} = \alpha_3 & \frac{S_2}{S_3} \frac{1-\gamma_b}{\gamma_b} \frac{P_4}{2\sqrt{x_{4,eq}}} \\ \frac{S_1}{S_4} \frac{1-\gamma_a}{\gamma_a} \frac{P_3}{2\sqrt{x_{3,eq}}} & \frac{P_4}{2\sqrt{x_{4,eq}}} = \alpha_4 \end{bmatrix} \begin{bmatrix} \delta x_3 \\ \delta x_4 \end{bmatrix} (t) + \\
 &+ \begin{bmatrix} 0 & \frac{S_2}{S_3} \frac{1-\gamma_b}{\gamma_b} \frac{P_2}{2\sqrt{x_{2,eq}}} \\ \frac{S_1}{S_4} \frac{1-\gamma_a}{\gamma_a} \frac{P_1}{2\sqrt{x_{1,eq}}} & 0 \end{bmatrix} \begin{bmatrix} \delta x_1 \\ \delta x_2 \end{bmatrix} (t) + \begin{bmatrix} d_3 \\ d_4 \end{bmatrix} (t), \begin{bmatrix} \delta x_3 \\ \delta x_4 \end{bmatrix} (0) = \begin{bmatrix} \delta x_{30} \\ \delta x_{40} \end{bmatrix}
 \end{aligned} \quad (22)$$

where the disturbance entering zero dynamics holds

$$\begin{bmatrix} d_3 \\ d_4 \end{bmatrix} = \begin{bmatrix} q_{d3} - \frac{S_2}{S_3} \frac{1-\gamma_b}{\gamma_b} q_{d2} \\ q_{d4} - \frac{S_1}{S_4} \frac{1-\gamma_a}{\gamma_a} q_{d1} \end{bmatrix}. \quad (23)$$

The following Lemma is concerned with stability of equation (20).

Lemma 1. Equation (20) is asymptotically stable (AS) if and only if

$$\beta(\gamma) = \gamma_a \gamma_b \left(\frac{S_3 S_4}{S_1 S_2} - 1 \right) + \gamma_a + \gamma_b - 1 > 0, \quad (24)$$

and in the uniform case $S = S_k$ and $\alpha_3 = \alpha_4 = \alpha$ the roots are

$$\lambda_1 = -K_1 < 0, \lambda_2 = -K_2 < 0, \lambda_{3,4} = -a \left(1 \pm \sqrt{1 + \frac{1-\gamma_a-\gamma_b}{\gamma_a \gamma_b}} \right). \quad (25)$$

Proof. The characteristic polynomial of the state matrix in (20) holds

$$\begin{aligned}
 P(\lambda) &= \lambda^2 + a_1 \lambda + a_0 = \lambda^2 + \lambda(\alpha_3 + \alpha_4) + \alpha_3 \alpha_4 \left(1 - \frac{1-\gamma_b}{\gamma_b} \frac{1-\gamma_a}{\gamma_a} \frac{S_2}{S_3} \frac{S_1}{S_4} \right) = \\
 &= \lambda^2 + \lambda(\alpha_3 + \alpha_4) + \frac{\alpha_3 \alpha_4}{\gamma_b \gamma_a} \frac{S_1 S_2}{S_3 S_4} \beta(\gamma)
 \end{aligned} \quad (26)$$

Since $a_1 = \alpha_3 + \alpha_4 > 0$, only the zero-order coefficient a_0 has undefined sign because of $\beta(\gamma)$. Under (22) both signs are positive and both roots have negative real part. Under equality as in (14) a zero root appears. At least one root has positive real part if $\beta(\gamma) < 0$. ■

Using Lemma 1 and the admissible set expression (18), we prove that the ideal control law (17) cannot usually stabilize equation (2) except when the critical coefficient $\beta(\gamma)$ is positive.

Theorem 1. Assume as initial condition of (20) a perturbed equilibrium state $x_{eq} + \delta x(0)$, such that the pair (x_{eq}, q_{eq}) satisfies (12) and the perturbation belongs to an open sphere $O(\epsilon) = \{\delta x(0), |\delta x(0)| < \epsilon\}$ with $\epsilon > 0$ arbitrarily small. For $\beta(\gamma) < 0$, there always exist an open subset $S(\epsilon) \subseteq O(\epsilon)$ such that at least one of the components $x_k, k = 3, 4$ diverges in a finite time t_1 up to $x_k(t) = x_{k,max}, t \geq t_1$, and, in the uniform case $S_k = S$, $a_k = a$ and $x_{k,max} = x_{max}$, moves the pair (x, q) into the empty admissible set \mathbf{A}_{sat} of (18).

Proof. Assume $\beta(\gamma) < 0$, and denote the positive eigenvalue of (20) with $\lambda_4 = p_4 > 0$ and the negative with $\lambda_3 = -p_3 < 0$. The free response of (20) can be written as

$$\begin{aligned}
x_1(t) &= x_{1,eq} + e^{-K_1 t} \delta x_1(0) \\
x_2(t) &= x_{2,eq} + e^{-K_2 t} \delta x_2(0) \\
x_3(t) &= x_{3,eq} + \delta_{31} e^{-K_1 t} + \delta_{32} e^{-K_2 t} + \delta_{33} e^{-p_3 t} + \delta_{34} e^{p_4 t}, \\
x_4(t) &= x_{4,eq} + \delta_{41} e^{-K_1 t} + \delta_{42} e^{-K_2 t} + \delta_{43} e^{-p_3 t} + \delta_{44} e^{p_4 t}
\end{aligned} \tag{27}$$

where all the coefficients $\delta_{jk}, j = 1, 2, 3, 4, k = 3, 4$ are functions of $\delta x(0)$. Any $\delta_{34} > 0$ and $\delta_{44} > 0$ forces x_3 and x_4 , respectively, to diverge toward saturation, since for $\beta(\gamma) < 0$, (20) is unstable for any x_{eq} . Saturation is met at t_1 defined by

$$\ln \frac{x_{k,max} - x_{k,eq}}{\delta_{k4}} \leq p_k t_1 \leq \ln \frac{x_{k,max} - x_{k,eq} + \sum_{j=1}^3 |\delta_{kj}|}{\delta_{k4}}. \tag{28}$$

Saturation implies the empty admissible set A_{sat} . ■

For this reason, stabilization in [23] has been approached by defining a new set of controllable state variables which under feedback linearization, exhibit relative degree two with respect to command q . In other words, we look into a pair of second-order linear equations in normal form (a series of two integrators) which is controllable by q and therefore is free of zero dynamics.

2.4. Problem B: the normal form of state equations and the ideal control law

The state equation of Problem B is obtained by taking the first and second derivative of (1). After some computations in the Appendix, the following state equation is found

$$\begin{aligned}
\dot{r}(t) &= A_r r(t) + B_r(x) q(t) + G_r(h_r(x) + d_r(t)), r(0) = r_0, \\
y_r(t) &= C_r r(t) + e_{mr}(t)
\end{aligned} \tag{29}$$

together with the following vectors and matrices

$$\begin{aligned}
r &= \begin{bmatrix} r_1 \\ r_2 \\ v_1 \\ v_2 \end{bmatrix} = \begin{bmatrix} r_{12} \\ v_{12} \end{bmatrix}, h = \begin{bmatrix} h_{r1} \\ h_{r2} \end{bmatrix}, d_r = \begin{bmatrix} d_{r1} \\ d_{r2} \end{bmatrix}, y_r = \begin{bmatrix} y_{r1} \\ y_{r2} \end{bmatrix}, G_r = \begin{bmatrix} 0 \\ I \end{bmatrix} \\
A_r &= \begin{bmatrix} 0 & 0 & 1 & 0 \\ 0 & 0 & 0 & 1 \\ 0 & 0 & 0 & 0 \\ 0 & 0 & 0 & 0 \end{bmatrix} = \begin{bmatrix} 0 & I \\ 0 & 0 \end{bmatrix}, B_r(x) = \begin{bmatrix} 0 & 0 \\ 0 & 0 \\ B_{r11}(x) & B_{r12}(x) \\ B_{r21}(x) & B_{r22}(x) \end{bmatrix} = \begin{bmatrix} 0 \\ B_{r2}(x) \end{bmatrix} \\
C_r &= \begin{bmatrix} 1 & 0 & 0 & 0 \\ 0 & 1 & 0 & 0 \end{bmatrix} = \begin{bmatrix} I & 0 \end{bmatrix}
\end{aligned} \tag{30}$$

The matrix $B_{r2}(x)$ is singular for

$$\left(1 - \frac{1}{\gamma_a}\right) \left(1 - \frac{1}{\gamma_b}\right) = \left(1 - \frac{P_1}{P_4} \sqrt{\frac{x_4}{x_1}}\right) \left(1 - \frac{P_2}{P_3} \sqrt{\frac{x_3}{x_2}}\right), \tag{31}$$

which corresponds to a set of hyperbola in the positive quadrant of the pair $(x_4/x_1, x_3/x_2)$, parameterized by γ . Since $\gamma_a \leq 1$ and $\gamma_b \leq 1$, invertibility is guaranteed by the pair of inequalities

$$\sqrt{x_1} > \frac{P_1}{P_4} \sqrt{x_4}, \sqrt{x_2} > \frac{P_2}{P_3} \sqrt{x_3}, \tag{32}$$

which demands the upper tank level not to be excessive as already pointed out by the empty set \mathbf{A}_{sat} in (18).

For later use, we need the following relation between r in (25) and x in (3):

$$\begin{aligned} r = \begin{bmatrix} r_{12} \\ v_{12} \end{bmatrix} &= \begin{bmatrix} F_{r1}x_{12} + F_{r2}x_{34} \\ F_{r1}f_{12}(x_{12}, x_{34}) + F_{r2}f_{34}(x_{34}) \end{bmatrix} + \begin{bmatrix} 0 \\ d_{12} \end{bmatrix}, \\ f_{12} &= \begin{bmatrix} -p_1 + p_3 \\ -p_2 + p_4 \end{bmatrix}, f_{34} = \begin{bmatrix} -p_3 \\ -p_4 \end{bmatrix} \\ d_{12} &= F_{r1} \begin{bmatrix} q_{d1} \\ q_{d2} \end{bmatrix} + F_{r2} \begin{bmatrix} q_{d3} \\ q_{d4} \end{bmatrix} \end{aligned} \quad (33)$$

Equation (26) is nonlinear and affected by the unknown disturbance d_{12} . The command q is cancelled on the purpose due to $F_{r1}B_{12} + F_{r2}B_{34} = 0$.

The ideal control law of (24), assuming $B_{r2}(x)$ invertible, has the following form

$$\begin{aligned} B_{r2}(x)q(t) &= -h(x) - d(t) + Ke_{r,ref}(t) \\ K &= [K_r \quad K_v], \quad e_{ref}(t) = r_{ref}(t) - r(t) \\ r_{ref}(t) &= \begin{bmatrix} z_{3,ref} = r_{1,ref} \\ z_{4,ref} = r_{2,ref} \\ 0 \\ 0 \end{bmatrix} = \begin{bmatrix} r_{12,ref}(t) \\ 0 \end{bmatrix} \end{aligned} \quad (34)$$

Lemma 2. Assume that K makes $A - G_r K$ asymptotically stable. The ideal control law (34) applied to (24) makes the tracking error $e_r(t)$ to be bounded, and if the reference $r_{ref}(t)$ is constant, asymptotically converging to zero.

Proof. Let us write the tracking error equation

$$\begin{aligned} \dot{e}_{ref}(t) &= (A_r - G_r K)e_{ref}(t) + \begin{bmatrix} 0 \\ \dot{r}_{12,ref}(t) \end{bmatrix}, e_{ref}(0) = e_{ref,0} \\ G_r &= \begin{bmatrix} 0 \\ I \end{bmatrix} = B_r(x)B_{r1}^{-1}(x) \end{aligned} \quad (35)$$

and remember that the reference derivative has been assumed to be bounded. Which proves the Lemma. ■

The question is whether Lemma 2 might be transferred to the lower tank levels, i.e. to the performance $z_{12} = x_{12}$. It will be proved that Lemma 2 holds if and only if no unknown disturbance exists, i.e. $q_d = 0$ in (2). More precisely, the tracking error is bounded if the unknown disturbance is bounded, but the error does not converge to zero even if the reference remains constant. To this end, let us build up the Jacobian $F(x)$ of the state dependent term of the relation between r and x in (26):

$$\begin{aligned} F(x) &= \begin{bmatrix} F_{r1} & F_{r2} \\ F_{r1} \frac{\partial f_{12}}{\partial x_{12}} & F_{r1} \frac{\partial f_{12}}{\partial x_{34}} + F_{r2} \frac{\partial f_{34}}{\partial x_{34}} \end{bmatrix} = \begin{bmatrix} F_{r1} & F_{r2} \\ F_{r1} \frac{\partial f_{12}}{\partial x_{12}} & (F_{r1} - F_{r2}) \frac{\partial f_{12}}{\partial x_{34}} \end{bmatrix} \\ \frac{\partial f_{12}}{\partial x_{12}} &= \frac{1}{2} \begin{bmatrix} -\frac{p_1}{\sqrt{x_1}} & 0 \\ 0 & -\frac{p_2}{\sqrt{x_2}} \end{bmatrix}, \frac{\partial f_{12}}{\partial x_{34}} = \frac{1}{2} \begin{bmatrix} \frac{p_3}{\sqrt{x_3}} & 0 \\ 0 & \frac{p_4}{\sqrt{x_4}} \end{bmatrix} \end{aligned} \quad (36)$$

The determinant of $F(x)$ satisfies the following Lemma.

Lemma 3. The Jacobian matrix $F(x)$ is singular for one of the three following equalities

$$\begin{aligned} \gamma_a &= 1 \\ \gamma_b &= 1 \\ \left(1 - \frac{1}{\gamma_a}\right) \left(1 - \frac{1}{\gamma_b}\right) &= \left(1 - \frac{P_1}{P_4} \sqrt{\frac{x_4}{x_1}}\right) \left(1 - \frac{P_2}{P_3} \sqrt{\frac{x_3}{x_2}}\right) \end{aligned} \quad (37)$$

The former two equalities rule out the case in which either lower tank level is dropped from the performance r . The third one is the same as the equality (31) which makes singular $B_{r2}(x)$. ■

We can now state the following Theorem.

Theorem 2. Assume that $A_r - G_r K$ in (35) is asymptotically stable, that the reference $r_{ref}(t)$ is constant and that the Jacobian matrix $F(x)$ in (29) is invertible, i.e. $|F^{-1}(x)| < \infty$ for any reachable x_{ref} defined by $r_{ref} = F_r x_{ref}$. Then the tracking error $e_{x,ref} = x_{ref} - x$ of the tank levels asymptotically converges to zero if and only if $\lim_{t \rightarrow \infty} d_r(t) = 0$.

Proof. First we convert relation (26) into a tracking error relation by expanding the nonlinear relation around the reference level x_{ref} . The expansion holds

$$\begin{aligned} e_{x,ref}(t) + d_r(t) &= F(x_{ref})e_{x,ref} + o(|e_{x,ref}|^2) \\ e_{x,ref} = x_{ref} - x, d_r &= \begin{bmatrix} 0 \\ d_{12} \end{bmatrix}, |o(|e_{x,ref}|^2)| \leq \eta |e_{x,ref}|^2 \end{aligned} \quad (38)$$

Assuming $|F^{-1}(x)| < \infty$, we can convert (31) into the two-sided norm inequality

$$\frac{|e_{ref}(t) + d_r(t)|}{|F(x_{ref})| + \eta |e_{x,ref}|} \leq |e_{x,ref}| \leq \frac{|e_{ref}(t) + d_r(t)|}{|F^{-1}(x_{ref})|^{-1} - \eta |e_{x,ref}|} \quad (39)$$

Then applying Lemma 2, sufficient and necessary conditions for $\lim_{t \rightarrow \infty} |e_{x,ref}| = 0$ are that $A_r - G_r K$ is AS, $\lim_{t \rightarrow \infty} d_r(t) = 0$ and that $r_{ref}(t)$ is constant. ■

In conclusion, disturbance rejection of the ideal control law (34) when applied to the tank combination r_{12} in (1) is not sufficient to reject unknown disturbances (including parametric errors) affecting lower and upper tanks.

3. Control algorithms and design

In this section the ideal control laws (17) (Problem A) and (34) (Problem B) will be designed and tuned according to the Embedded Model Control.

First the discrete-time (DT) embedded model will be derived as a combination of controllable and disturbance dynamics. The latter dynamics, driven by arbitrary signals to be estimated (noise), is necessary to predict and reject unknown disturbance. We will prove that noise may drive any state variable as in the extended state observers (ESO), but only the state variables whose equation is affected by uncertainty. This implies that the output to state feedback around the embedded model cannot be always static as in the ESO, but it may be dynamic. The reason is that such a feedback (noise estimator), driven by the model error is just in charge of estimating noise. The ensemble of noise

estimator and embedded model plays the role of a state predictor, which supplies state predictions to control law.

Noise estimator gains are tuned by fixing the closed-loop eigenvalues in the presence of the uncertainty sets (disturbance, parametric, neglected dynamics, measurement errors). The goal is to guarantee BIBO stability and to achieve accuracy requirements in the presence of uncertainty. Asymptotic expansion of the state predictor sensitivity is the adopted way.

The adopted control laws are just the ideal laws where all the input variables are replaced by those provided by state predictors. Control law must be accompanied by a reference generator capable of smoothing the reference trajectories, so as to respect actuator limits and tracking error bounds. The subject is not detailed here for brevity's sake. The feedback gains K in (19) and (34) are designed by fixing the eigenvalues of the closed-loop state matrices in (20) and (35). The corresponding frequency BW f_{ck} will be wider than the state predictor one f_{mk} , not to disturb state predictor design.

3.1. Problem A: embedded model, state predictor and control law

Four decoupled embedded models are designed, one for each tank level measurement $y_k(i)$ in (3). To account for the disturbance dynamics in (5), each state equation is third order. The only interconnection occurs via the nonlinear function $h_k(x)$ which is cancelled by the control law. The k -th embedded model is the following

$$\begin{aligned} \begin{bmatrix} x_k \\ x_{dk} \\ x_{sk} \end{bmatrix} (i+1) &= \begin{bmatrix} 1 & 1 & 0 \\ 0 & 1 & 1 \\ 0 & 0 & 1 \end{bmatrix} \begin{bmatrix} x_k \\ x_{dk} \\ x_{sk} \end{bmatrix} (i) + \begin{bmatrix} b_k \\ 0 \\ 0 \end{bmatrix} u_k(i) + \begin{bmatrix} h_k(x) \\ 0 \\ 0 \end{bmatrix} + w_k(i) \\ y_k(i) &= x_k(i) + e_{mk}(i), \begin{bmatrix} x_k \\ x_{dk} \\ x_{sk} \end{bmatrix} (0) = \begin{bmatrix} x_{k,0} \\ x_{dk,0} \\ x_{sk,0} \end{bmatrix}, w_k = \begin{bmatrix} w_{uk} \\ w_{dk} \\ w_{sk} \end{bmatrix} \end{aligned} \quad (40)$$

where command $b_k u_k$, h_k and the overall disturbance d_k are defined by

$$\begin{aligned} \begin{bmatrix} u_1 \\ u_2 \\ u_3 \\ u_4 \end{bmatrix} &= T \begin{bmatrix} \frac{\gamma_a}{s_1} q_a \\ \frac{\gamma_b}{s_2} q_b \\ \frac{1-\gamma_b}{s_3} q_b \\ \frac{1-\gamma_a}{s_4} q_a \end{bmatrix}, \begin{bmatrix} h_1 \\ h_2 \\ h_3 \\ h_4 \end{bmatrix} (x) = T \begin{bmatrix} -p_{1,nom}(x_1) + p_{3,nom}(x_3) \\ -p_{2,nom}(x_2) + p_{4,nom}(x_4) \\ -p_{3,nom}(x_3) \\ -p_{4,nom}(x_4) \end{bmatrix}. \\ d_k(i) &= x_{dk}(i) + h_k(x) + w_{uk}(i) \end{aligned} \quad (41)$$

The subscript *nom* indicates that nominal parameters are used. Parametric errors are hidden in the disturbance dynamics. Equation (33) is unstable and not stabilizable in agreement with the parameter-free dynamics (5). Actuator and sensor delays have been neglected and confined into the fractional error dynamics E_k . By using Z-transfer functions, by denoting the embedded model and the 'truth' transfer functions with $M_k(z) = y_{mk}/u_k$ and $P_k(z) = y_k/u_k$, respectively, E_k is defined by

$$E_k(z) = \frac{e_{mk}(z)}{y_{mk}(z)} = M_k^{-1}(z)P_k(z) - 1 = (1 + \partial b_k)(1 + \epsilon_k)z^{-\nu} - 1, \quad (42)$$

$$\nu T = \tau_u + \tau_y$$

where ν is the total delay in (2), ∂b_k and ϵ_k account for actuator and sensor scale factor uncertainty. Time unit T must be designed. Fig. 5 shows a typical polar plot of $E_k(e^{j\omega T})$ in (42).

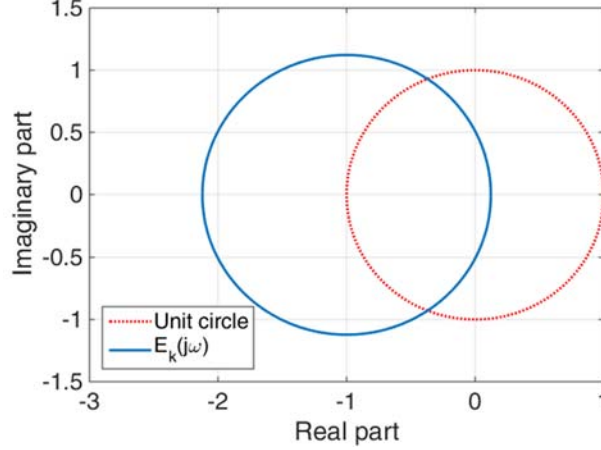


Fig. 5. Polar plot of E_k .

Since the state vector in (33) is observable by y_k , the k -th noise estimator may be decoupled from $j \neq k$, only driven by model error e_{mk} . Moreover, since state size $n_x = 3$ and noise size $n_w = 3$ are equal, feedback from model error to noise vector is just static as follows

$$w_k(i) = L_k e_{mk}(i), L_k = \begin{bmatrix} l_{uk} \\ l_{dk} \\ l_{sk} \end{bmatrix}. \quad (43)$$

The three gains in (35) are designed by fixing the closed-loop spectrum $\Lambda_{mk} = \{\lambda_{mkj} = 1 - \gamma_{mkj}\}, j = 1, 2, 3$ of the state predictor which consists of (33) and (35), such that $|\lambda_{mkj}| < 1$. The parameter γ_{mkj} may be referred to as ‘DT complementary eigenvalue’ and approximates the relevant Fourier frequency f_{mkj} [Hz] as follows

$$\lim_{\gamma_{mkj} \rightarrow 0} f_{mkj} = \frac{\gamma_{mkj}}{2\pi T}. \quad (44)$$

The expression of L_k in terms of Λ_{mk} follows from the characteristic polynomial and holds

$$l_{uk} = \sum_{j=1}^3 \gamma_{mkj}, l_{dk} = \sum_{j=1}^2 (\gamma_{mkj} \sum_{h=j+1}^3 \gamma_{mkh}), l_{sk} = \prod_{j=1}^3 \gamma_{mkj}. \quad (45)$$

State predictions $x_k(i+1)$, $k = 1, 2, 3, 4$, and $x_{dk}(i+1)$, $k = 1, 2$ allow to pre-compute the control law (17) as follows

$$u_k(i+1) = u_{k,ref}(i) + b_k^{-1} \left(K_k e_{k,ref}(i+1) - h_k(x(i+1)) - x_{dk}(i+1) \right), \quad (46)$$

$$e_{k,ref}(i+1) = x_{k,ref}(i) - x_k(i+1), k = 1, 2$$

Equation (39) only aims to the level regulation of the lower tanks, $k = 1, 2$, but $h_k(x)$ demands to predict the four-dimensional state x , which is provided by four state predictors. One may wonder whether the upper tank state predictors $k = 3, 4$ are necessary, since only x_k is employed, which may be replaced by the measurement y_k . As an answer, noise-free prediction is needed.

The reference command $u_{k,ref}$ is the output of a smoothing reference generator

$$x_{k,ref}(i+1) = x_{k,ref}(i) + u_{k,ref}(x_{k,ref}(i), z_{k,ref}(i)), x_{k,ref}(0) = x_{k,ref,0} \quad (47)$$

where $u_{k,ref}(\cdot)$ is a nonlinear function capable of matching reference trajectories $z_{k,ref}(i)$ with the admissible set $\mathbf{A}(\gamma)$.

3.2. Problem B: embedded model, state predictor and control law

The four state predictors which consists of (33) and (35) remain valid also in this case since we need the prediction of x for computing $h(x)$ and $B_v(x)$ in (34). In addition, we need the embedded model of (24) for computing $r(t)$ and $d(t)$ in (34). Two state-decoupled fourth-order DT state equations $j = 1, 2$ derive from (24) and (5). In practice we need to describe a series of two integrators driven by command and a second order disturbance as in (5). Equations are interconnected by x and the command vector $u = q$. The bivariate embedded model reads as

$$\begin{aligned} \begin{bmatrix} r \\ \Delta r \\ x_d \\ x_s \end{bmatrix} (i+1) &= \begin{bmatrix} I & I & 0 & 0 \\ 0 & I & I & 0 \\ 0 & 0 & I & I \\ 0 & 0 & 0 & I \end{bmatrix} \begin{bmatrix} r \\ \Delta r \\ x_d \\ x_s \end{bmatrix} (i) + \begin{bmatrix} 0 \\ B(x) \\ 0 \\ 0 \end{bmatrix} u(i) + \begin{bmatrix} 0 \\ h(x) \\ 0 \\ 0 \end{bmatrix} + Gw(i) \\ y(i) &= r(i) + e_m(i), \begin{bmatrix} r \\ \Delta r \\ x_d \\ x_s \end{bmatrix} (0) = \begin{bmatrix} r \\ \Delta r \\ x_d \\ x_s \end{bmatrix} \end{aligned} \quad (48)$$

where $I = I_2$, $\Delta r_j = v_j T$ is a level increment, and matrices and vectors hold

$$\begin{aligned} B(x) &= T^2 B_{r2}(x), h(x) = T^2 h_r(x) \\ w &= \begin{bmatrix} w_u \\ w_d \\ w_s \end{bmatrix}, G = \begin{bmatrix} 0 & 0 & 0 & 0 \\ 0 & I & 0 & 0 \\ 0 & 0 & I & 0 \\ 0 & 0 & 0 & I \end{bmatrix}. \end{aligned} \quad (49)$$

The noise estimator cannot be static since the state size $n_x = 4 \times 2$ is larger than the noise size $n_w = 3 \times 2$. The reason comes from respecting the noise-free kinematic relation in (24), $\dot{r} = v$, which has been converted into $r(i+1) = r(i) + \Delta r(i)$. The minimal order of the dynamic feedback is $(n_x - n_w)/2 = 1$ [28], [29], which leads to the estimator

$$\begin{aligned} x_e(i+1) &= (1 - \beta)x_e(i) + e_m(i), x_e(0) = x_{e0} \\ w(i) &= Nx_e(i) + Le_m(i), L = \begin{bmatrix} L_u \\ L_d \\ L_s \end{bmatrix}, N = \begin{bmatrix} N_{uj} \\ N_{dj} \\ N_{sj} \end{bmatrix}. \end{aligned} \quad (50)$$

The resulting state predictor which consists of (44) and (46) is fifth-order. The

relation between the closed-loop spectrum Λ_{mj} and the gains in (46) can be found in [28] and [29].

The bivariate ideal control law (34), by assuming $B(x)$ invertible, converts into

$$\begin{aligned} B(x)u(i+1) &= B(x)u_{ref}(i) + Ke_{ref}(i+1) - h(x) - x_d(i+1) \\ K &= [K_r \quad K_v], \quad e_{ref}(i+1) = \begin{bmatrix} r_{ref}(i) - r(i+1) \\ \Delta r_{ref}(i) - r(i+1) \end{bmatrix} \end{aligned} \quad (51)$$

The reference command u_{ref} and the reference level increment Δr_{ref} are the output of a smoothing reference generator as in (40).

3.3. Problem A: pole placement

Consider a single lower tank level, $k = 1, 2$. It has been shown in [26] that the tracking error equation takes the form

$$\begin{aligned} e_k(i+1) &= \begin{bmatrix} 1-l_{xk} & 1 & 0 & 0 \\ -l_{dk} & 1 & 1 & 0 \\ -l_{sk} & 0 & 1 & 0 \\ -l_{xk} & 0 & 0 & 1-K_k \end{bmatrix} e_k(i) - \begin{bmatrix} l_{xk} \\ l_{dk} \\ l_{sk} \\ -l_{xk} \end{bmatrix} (e_{mk}(i) + d_{yk}(i)) \\ e_{k,ref}(i) &= [1 \quad 0 \quad 0 \quad -1] e_k(i) + d_{yk}(i), \quad e_k(0) = e_{k0} \end{aligned} \quad (52)$$

where e_k is the state vector and d_{yk} is the total disturbance d_k in (34) when shifted to the output, which in this case is achieved by simple integration. The state matrix in (52) is the combination of the state predictor matrix (the upper 3×3 diagonal block) and of the command state feedback $1 - K_k$ (the lower scalar diagonal block). In terms of Z transfer functions, (41) becomes

$$e_{k,ref}(z) = -V_k(z)e_{mk}(z, \mathbf{E}, \mathbf{W}_y) + S_k(z)d_{yk}(z, \mathbf{D}, \mathbf{\Pi}), \quad (53)$$

where S_k is the overall closed-loop sensitivity (low-pass filter) and $V_k = 1 - S_k$ is the complementary sensitivity (high-pass filter, the ‘complement’ for short). Equations (50) and (51) are driven by uncertainty as explicitly indicated in (53)(51). Robust stability versus \mathbf{E} (neglected dynamics defined in (42)) is guaranteed by the high-frequency decay of $|V_k(e^{j\pi f T})| = |V_k(jf)|$. Performance as in (9) is guaranteed by the low-frequency asymptote of $|S_k(jf)|$. An asymptotic design procedure has been proved and shown in [32]. The following low- and high-frequency asymptotes derive from (52) and (45) under the assumption of coincident state-predictor spectrum $\Lambda_{mk} = \{\lambda_{mkj} = 1 - \gamma_{mk}\}, j = 1, 2, 3$:

$$\begin{aligned} V_{\infty k}(z) &= \lim_{(z-1) \rightarrow \infty} V_k(z) = \frac{l_{dk} + K_k l_{uk}}{(z-1)^2} = \left(\frac{\gamma_{mk}}{z-1}\right)^2 3 \left(1 + \frac{K_k}{\gamma_{mk}}\right) \\ S_{0k}(z) &= \lim_{(z-1) \rightarrow 0} S_k(z) = (z-1)^3 \frac{K_k + l_{uk}}{K_k l_{sk}} = \left(\frac{z-1}{\gamma_{mk}}\right)^3 \left(1 + 3 \frac{\gamma_{mk}}{K_k}\right). \end{aligned} \quad (54)$$

The limit for $(z-1) \rightarrow \infty$ searches asymptotes of the kind $K_{\infty}(z-1)^{-r}$, where $r > 0$ is the relative degree of $V_k(z)z^m$ and $m \geq 0$ is the delay degree. In other terms, delays are excluded. By replacing the Fourier frequency defined in (44), the approximate frequency domain asymptotes follow

$$\begin{aligned} |V_{\infty k}(jf)| &\cong \left(\frac{f_{mk}}{f}\right)^2 3 \left(1 + \frac{f_{ck}}{f_{mk}}\right), \lim_{K_k \rightarrow 0} f_{ck} = \frac{K_k}{2\pi T}, \\ |S_{0k}(jf)| &\cong \left(\frac{f}{f_{mk}}\right)^3 \left(1 + 3 \frac{f_{mk}}{f_{ck}}\right), \end{aligned} \quad (55)$$

where equalities tend to be exact for $\gamma_{ck} \rightarrow 0$ and $\gamma_{mk} \rightarrow 0$. The intersection frequencies with the 0dB axis hold

$$f_{ck,0} \cong f_{mk} \sqrt{3 \left(1 + \frac{f_{ck}}{f_{mk}}\right)} > f_{mk,0} \cong \frac{f_{mk}}{\sqrt[3]{1 + 3 \frac{f_{mk}}{f_{ck}}}} \quad (56)$$

The frequencies $f_{mk,0}$ and $f_{ck,0}$ play the role of the state predictor and of the command state feedback bandwidths, respectively. Time unit T enters (56)(55) through (44) and (55), in other terms both frequencies are bounded by the Nyquist frequency $f_{max} = 0.5T^{-1}$.

The first design step demands the state predictor, which has the narrower BW in (56), to guarantee the settling time τ_s in (9). The second step demands that $f_{ck} \gg f_{mk}$, i.e. not to narrow $f_{mk,0}$ in (56). The third step fixes $f_{max} > f_{ck}$ for avoiding excessive command authority. By adopting as a first trial the rule of thumb of one order of magnitude, we summarize the above findings as

$$\kappa f_s \leq f_{mk} \leq \frac{f_{ck}}{\kappa} \leq \frac{f_{max}}{\kappa^2}, \kappa \approx 10, f_s = \frac{1}{2\pi\tau_s}. \quad (57)$$

Up to now no uncertainty set has been used. The next step is to fix another lower bound to f_{mk} in order to guarantee accuracy (9) in the presence of \mathbf{D} and \mathbf{W}_y . Focusing on \mathbf{D} , the low-frequency asymptote $S_{0k}(jf)$ in (55) being third-order is such to reduce a third-order drift (or a piecewise parabola) to a residual white noise (or to an arbitrary zero-mean signal). In fact, \mathbf{D} has been assumed as a class of second-order dynamics in (5), which becomes third order after integration in order to obtain the output disturbance d_{yk} in (41). For instance, a third-order drift of d_{yk} having high-frequency (unilateral) spectral density (PSD for short hereinafter)

$$S_d^2(f) = S_{d0}^2 \left(\frac{f_d}{f}\right)^6, \quad (58)$$

is reduced to a residual noise with constant spectral density

$$S_w^2(f) \cong |S_{0k}(jf)|^2 S_{d0}^2 \left(\frac{f_d}{f}\right)^6 \cong S_{d0}^2 \left(\frac{f_d}{f_{mk}}\right)^6 \left(1 + 3 \frac{f_{mk}}{f_{ck}}\right)^2 \quad (59)$$

Further, by assuming the tracking error to be dominated by the residual noise after the settling time, we may convert (9) into

$$\sqrt{\text{var}(e_{k,ref})} \leq \frac{e_{k,max}}{3} = \rho_k, t_j + \tau_s \leq t < t_{j+1}, \quad (60)$$

where ρ_k is the output quantization level defined in (7). The variance of (59) inserted in (60), yields the implicit bound

$$f_{mk} \geq f_d \sqrt[3]{\left(1 + 3 \frac{f_{mk}}{f_{ck}}\right) \frac{S_{d0} \sqrt{f_{max}}}{\rho_k}}, \quad (61)$$

which is to be added to (57).

The last step is to guarantee closed-loop stability in presence of \mathbf{E} and $\mathbf{\Pi}$. In both cases, the effect is a further loop driven by the tracking error, which demands to rewrite (53) as

$$\begin{aligned} (1 + V_k(z)E_k(z) - S_k(z)\Pi_k(z))e_{k,ref}(z) = \\ = -V_k(z)e_{mk}(z, \mathbf{W}_y) + S_k(z)d_{yk}(z, \mathbf{D}) \end{aligned} \quad (62)$$

where E_k has been defined in (42) and Π_k is defined below. Closed-loop stability is guaranteed if the H_∞ inequality (from the gain theorem) holds

$$\max_{|f| < f_{\max}} (|V_k(jf)E_k(jf)| + |S_k(jf)\Pi_k(jf)|) \leq \eta < 1. \quad (63)$$

Since the terms in (63) insist on different frequency domains, (63) splits in two separate inequalities. Consider first the right term $|V_k E_k|$, which includes the neglected dynamics. As Fig. 5 shows $|E_k(jf)| \leq 2(1 + \delta_k)$, with $\delta_k = |\delta b_k| + |\epsilon_k|$, and the peak is achieved at $f \cong f_{\max}/v$. Using (55), the first stability inequality provides an upper bound to f_{ck} as follows

$$f_{ck} \leq f_{\max} \left(\frac{\eta}{3v^2} \phi_k - \phi_k^{-1} \right) \cong f_{\max} \frac{\eta}{3v^2} \phi_k, \phi_k = \frac{f_{\max}}{f_{mk}} \gg 1. \quad (64)$$

Finally, Π_k can be approximated by expanding the unknown part $\Delta h_k(x) = h_k(x) - h_{nom,k}(x)$ around the reference level as follows

$$\begin{aligned} \Delta h_k(x) &= \Delta h_k(x_{k,ref}) + \frac{\partial \Delta h_k}{\partial x}(x_{k,ref})e_{ref} \\ \frac{\partial \Delta h_k}{\partial x}(x_{k,ref}) &= T \frac{P_{k,nom}}{2\sqrt{x_{k,ref}}} \partial P_k = T2\pi f_k \partial P_k \end{aligned} \quad (65)$$

where $\tau_k(x_{k,ref}) = (2\pi f_k)^{-1}$ is the discharge time constant of the k -tank. Integration of (65) provides $\Pi_k(z) \cong T2\pi f_k \partial P_k (z-1)^{-1}$ and after some computation, the second stability inequality

$$f_{mk} \geq f_k \sqrt[3]{\frac{1+3\frac{f_{mk}}{f_{ck}}}{\eta^4}} \quad (66)$$

which is the third lower bound of f_{mk} to be added to (57).

Observe that the first stability inequality (64) is such to narrow the closed-loop BW, whereas the second inequality (66) is doing the opposite. These findings agree with the standard control design practice, where structural uncertainty like neglected dynamics (but not parametric uncertainty) demands the BW to be narrowed, whereas disturbance rejection (including parametric uncertainty) demands the BW to be widened as in the ADRC [24] and in the high-gain observer literature [35]. The main deviation is inequality (56), which by enlarging the ratio f_{ck}/f_{mk} simplifies to

$$f_{ck,0} \cong f_{mk} \sqrt[3]{3 \frac{f_{ck}}{f_{mk}}} > f_{mk,0} \cong f_{mk}. \quad (67)$$

On the same line, by fixing the ratio f_{\max}/f_{ck} , the first stability inequality (64) is

rewritten by pivoting on f_{mk} as follows

$$f_{mk} \leq f_{max} \frac{\eta}{3v^2} \frac{f_{max}}{f_{ck}}. \quad (68)$$

In summary, performance and stability inequalities are such to provide lower and upper bounds of the state predictor BW f_{mk} , where f_{ck} , $f_{max} > f_{ck}$ and $\eta < 1$ play the role of degrees of freedom. Such inequalities also show that the state predictor must be designed and tuned uncertainty-based. By collecting and simplifying (57), (61), (66) and (68), the final design inequality is found

$$\max \left\{ f_s \kappa, f_k \partial P_k \frac{1}{\sqrt[3]{\eta^4}}, f_d \sqrt[3]{\frac{S_{do} \sqrt{f_{max}}}{\rho_k}} \right\} \leq f_{mk} \leq f_{max} \frac{\eta}{3v^2} \frac{f_{max}}{f_{ck}}. \quad (69)$$

A two-sided inequality like (69), though to the authors' knowledge absent in the literature, is the key asset of Embedded Model Control, and may be converted into an optimization criterion [28]. Of course, (69) may result to be unfeasible, but increasing f_{max} and/or decreasing f_{ck} may allow the upper bound to be enlarged.

Pole placement for problem B follows the same procedure, although sensitivity and complementary asymptotes are somewhat more complicated. Embedded model (48) is the same as that of a two degree-of-freedom motion, so pole placement as in [28] applies.

4. Simulated results

Simulated results aim to confirm the proved theorems and the pole placement method in Section 3.3. First simulated data will be provided. Then problem A and problem B simulated runs are reported. This section ends with a discussion about results and developments.

4.1. Simulated parameters and control requirements

Parameters in Table 1 are very similar to those reported in [9]. The discharge time constant $\tau_k(x_0) = 2\sqrt{x_{k0}} P_{k,nom}^{-1}$ is computed at the initial tank level x_0 from (65).

Control requirements in (9) have been partly fixed in (60). The settling time τ_s is fixed of the same order of the discharge time constants in (70). In summary

$$\begin{aligned} \tau_s &\approx \tau_k(x_0) \\ e_{k,max} &= 3\rho_k \end{aligned} \quad (70)$$

Table 1. Simulated parameters and uncertainty				
Parameter symbol	Nominal value	(fractional) uncertainty	Unit	Description (equation No.)
$S_k, k = 1,2,3,4$	0.06	0.1	m ²	Tank cross-section (4)
$a_k, k = 1,2,3,4$	0.882~1.51	0.1	m ²	Discharge constant (3)
$x_k(0)$	0.65~0.66		m	Initial tank level (2)
$x_{k,max}, k = 1,2,3,4$	1.3~1.36		m	Maximum tank level (2)

$q_{j,max}, j = a, b$	0.9~1.1		dm ³ /s	Maximum pump flow (2)
$\rho_j, j = a, b$	0.9~1.0		cm ³ /s	Command quantization (6)
$\rho_k, k = 1, 2, 3, 4$	1.3		mm	Measurement quantization (7)
T	1		s	Simulation time unit (5)
f_{max}	0.5		Hz	Nyquist frequency (57)
νT	2	≤ 3	s	Total delay (42)
f_d	0.64~1	0	mHz	Disturbance frequency (58)
S_{d0}	1.9~3.2	0	m/ $\sqrt{\text{Hz}}$	Low frequency unilateral PSD (square root) (58)
$\tau(x_0)$	145~250		s	Discharge time constant at the initial tank level (65)
τ_s	200		s	Requirement: settling time (71)
$e_{k,max}$	3.9		mm	Requirement: maximum tracking error (71)

4.2. Problem A simulation runs

Control parameters are listed in Table 2 and are derived from the pole placement procedure in Section 3.3. Using values in Table 1 and Table 2, the two-sided inequality (69) becomes

$$\max\{0.8 \times 5, 1 \times 0.9, 1 \times 0.9\} = 4 \leq f_{mk} \leq 2 \frac{f_{max}}{f_{ck}} \text{ [mHz]}, \quad (71)$$

which demands $f_{ck} < f_{max}/2$ to be feasible. Starting from the lower bound in (71), a manual optimization has been performed for reducing the overshoot of the sensitivity magnitude according to [29] and [36]. The resulting sensitivity S_k and complement V_k are shown in Fig. 6. The same figure, right, shows the polar plots of the neglected dynamics before after being filtered by V_k .

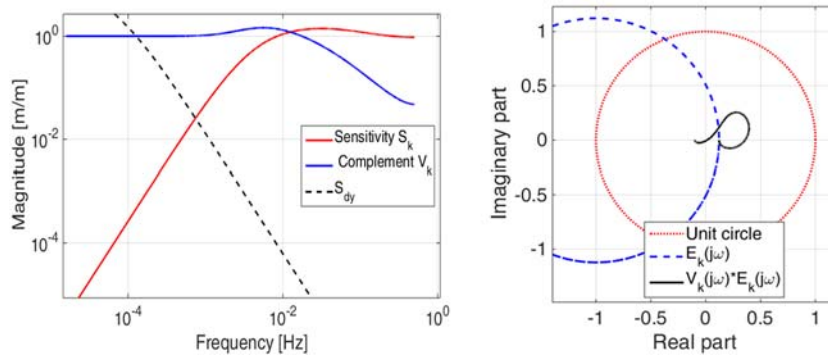


Fig. 6. Right: closed loop sensitivity, complement and S_d . Left: polar plot of the neglected dynamics before and after filtering.

Table 2. Problem A control parameters and performance			
Parameter symbol	Value	Unit	Description (equation No.)
T	1	s	Time unit
η^{-1}	3		Stability margin (63)
κ	5		Scale factor (69)
$\{\gamma_{mkj}, j = 1,2,3\}$	$\{0.05, 0.08, 0.1\}$		State predictor complementary eigenvalues
$f_{mk}, k = 1,2,3,4$	$\cong 0.013$	Hz	State predictor BW
$K_k, k = 1,2$	0.5		State feedback gain
f_{ck}	0.08	Hz	State feedback BW
τ_s	<200	s	Performance: settling time
$e_{k,max}$	<1	mm	Performance: maximum tracking error

Given a reference trajectory $z_{k,ref}(t), k = 1,2$ for each lower tank level in Table 3, an admissible trajectory $x_{k,ref}(t) \in \mathbf{A}(\gamma)$ is computed by the reference generator. Computation depends on the nominal fraction vector γ_{nom} , such that $\gamma = \gamma_{nom}(1 + \partial\gamma)$, where $\partial\gamma$ is the fractional uncertainty. Three cases A, B and C close to the critical condition $\beta(\gamma) = 0$ are presented. In the case A with $\beta(\gamma) = 0.1$ the four set points of $z_{k,ref}(t)$ are corrected to be admissible but do not coincide. In the case B with $\beta(\gamma) = 0.02$ they are forced to coincide because $\mathbf{A}(\gamma)$ is close to a line, but lower tank regulation is achieved. In the case B with $\beta(\gamma) < 0$, lower tank regulation fails as expected from Theorem 1, because an upper tank level reaches saturation.

Table 3. Set points [m] and γ for the simulated cases A, B and C					
Case	Initial level	Set point 1 (1,2)	Set point 2 (1,2)	Set point 3 (1,2)	(γ_a, γ_b)
Time [s]	0	3000	6000	9000	
Nominal	$(0.65, 0.66) \times 2$	$(0.3, 0.3)$	$(0.5, 0.75)$	$(0.9, 0.75)$	
A	$(0.65, 0.66) \times 2$	$(0.3, 0.3)$	$(0.5, 0.75)$	$(0.71, 0.60)$	$(0.5, 0.6)$
B	$(0.65, 0.66) \times 2$	$(0.87, 0.7)$	$(0.87, 0.7)$	$(0.87, 0.7)$	$(0.51, 0.51)$
C	$(0.65, 0.66) \times 2$	$(0.58, 0.5)$	$(0.58, 0.5)$	$(0.80, 0.66)$	$(0.48, 0.48)$
Fraction uncertainty $\partial\gamma = 0.05$					

Fig. 7, Fig. 8 and Fig. 9 refer to the Case A. Fig. 7, right, shows the four tank time history, where only lower tanks are regulated to their set points notwithstanding the highly irregular level (hence of the discharge flow) of the upper tanks. Fig. 7, left, shows that the lower tank levels move inside the admissible set.

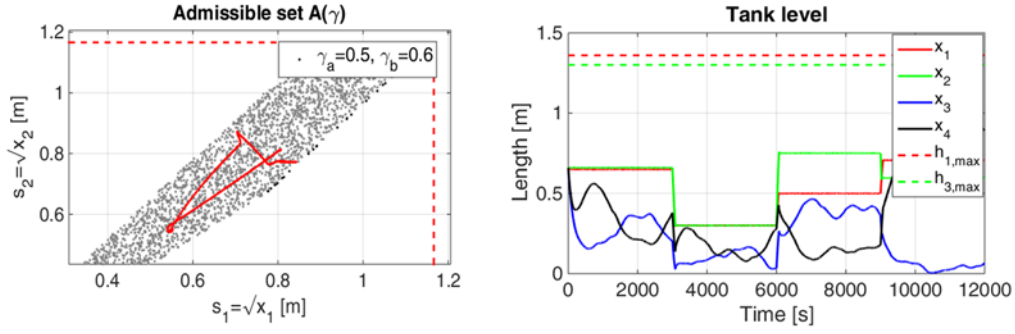


Fig. 7. Case A. Tank level time history. Left: admissible set and trajectory. Right: four tanks.

Fig. 8 shows the lower tank tracking error. At any set point change the error jumps because no reference smoothing has been applied to be conservative. Fig. 8, right, enlarges the tracking error between two set point changes. Both settling time and error tolerance meet the requirements as reported in Table 2, except in the last interval ($t > 10000s$) because of q_a saturation due to excessive disturbance. At steady state, the error is subject to a bounded zero-mean limit cycle due which is imposed by quantization and neglected dynamics (actuator and sensor delay).

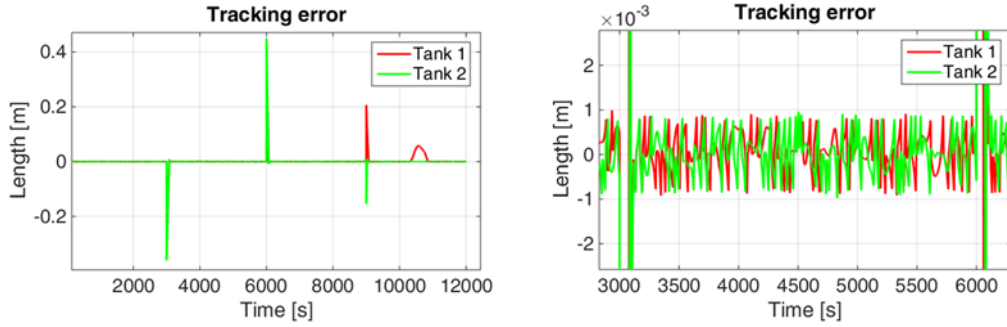


Fig. 8. Case A. Left tracking error for the lower tanks. Right: enlargement.

Fig. 9, left, shows the command flow history: saturation occurs because of the set point jumps as they are not mitigated by the reference generator. Fig. 9, right shows the unknown disturbance in flow units. Each component magnitude may reach about 5% of the maximum command flow.

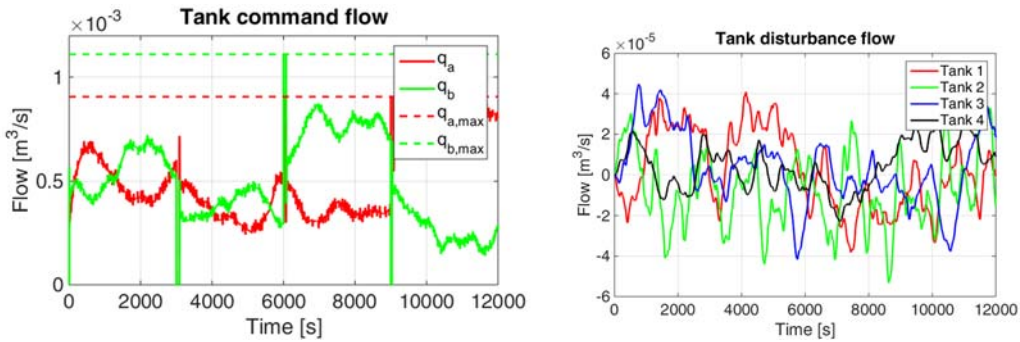


Fig. 9. Case A: Pump command flows and disturbance flows.

Fig. 10 shows the Case B trajectory of the lower tanks and the time history of the

four tanks. As Fig. 10, left, shows, initial conditions have been left on the purpose outside of the admissible set. At the end of the first interval close to 3000s, the upper tank 3 saturates and the tracking error accuracy is lost. But the next set point is forced to admissible and accuracy is fully recovered as shown in Fig. 11 when $q_a = 0$. In the Case B $\beta(\gamma) > 0$.

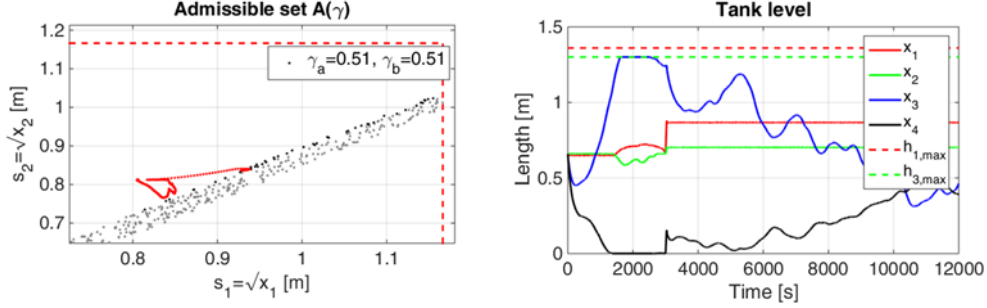


Fig. 10. Case B. the lower tank trajectory recovers the admissible set. Right: time history.

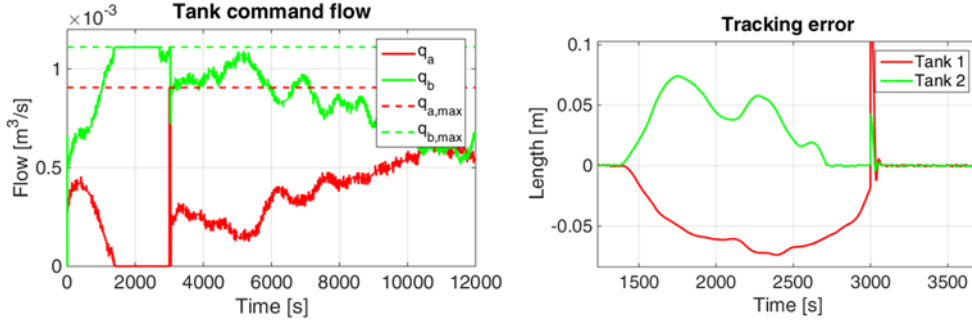


Fig. 11. Case B. Left: commanded pump flow. Right: tracking error.

Fig. 12 corresponds to the Case C where $\beta(\gamma) < 0$ and the zero dynamics is unstable. Though the lower tank trajectory is brought inside the admissible set as in Fig. 12, left, it remains, at least x_1 , for most of the time unregulated because $q_a = 0$, as expected from Theorem 1. Only after $t = 10000$ s, both tank levels are regulated to be accurate notwithstanding $x_3 = x_{3,max}$. The reason is that tank parameters are not uniform and the admissible set A_{sat} in (18) and Fig. 4 is not empty.

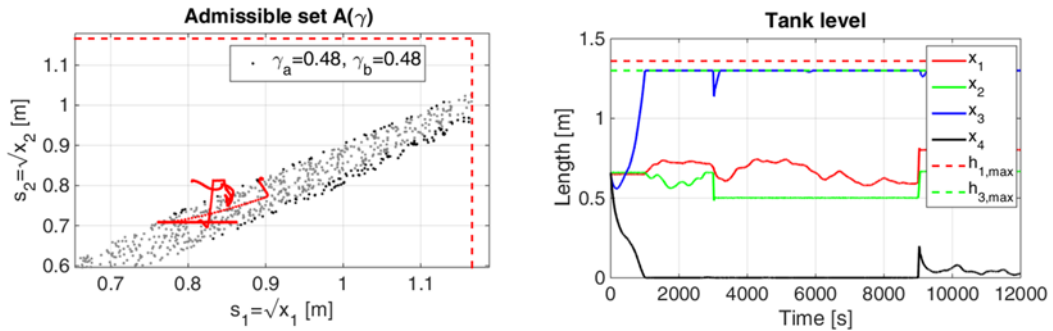


Fig. 12. Case C. Left: lower tank trajectory. Right: four tank level history.

4.3. Problem B simulation runs and discussion

Unlike Problem A, Problem B is capable of controlling the combined levels $r_k, k = 1, 2$ in (1) for any $\beta(\gamma)$. The five dimensional spectrum Λ_m of the state predictor (48) and (50) and the two dimensional feedback gain K in (51) have been designed to repeat Problem A sensitivity and complement S_k and V_k (see Fig. 6) in the mid frequency range as shown in Fig. 13. In fact, both low-frequency asymptote $S_{0k}(z)$ and high-frequency asymptote $V_{\infty k}(z)$, being steeper, cannot match those of Problem A. Being steeper, they should facilitate achievement of performance and stability inequality (63). Because of Theorem 2, such a statement, though partly applicable to the combined levels r_k , fails in the regards of the lower tank levels $x_k, k = 1, 2$. In fact it tends to fail also in the regards of r_k since an uncertainty on γ becomes a measurement scale factor error which cannot be recovered.

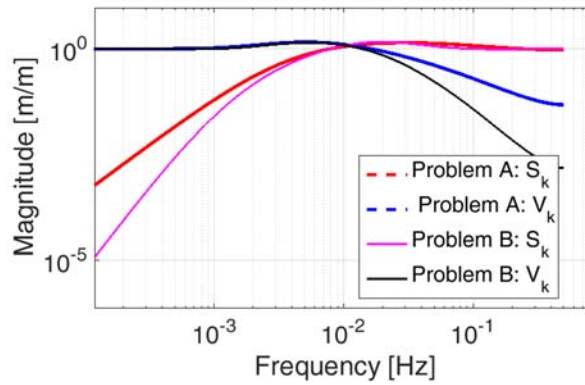


Fig. 13. Sensitivity and complement of both problems.

Also for Problem B no smoothing reference generator has been applied for comparison with Problem A. Simulated runs refer to a pair of cases. The Case A with $\beta(\gamma) > 0$ is the same as Problem A (see Table 3). The Case B with $\beta(\gamma) < 0$ is typical of Problem B.

Table 4. Lower tank set points [m] and γ for the simulated cases A and B					
Case	Initial level	Set point 1 (1,2)	Set point 2 (1,2)	Set point 3 (1,2)	(γ_a, γ_b)
Time [s]	0	3000	6000	9000	
A	$(0.65, 0.66) \times 2$	$(0.3, 0.3)$	$(0.5, 0.75)$	$(0.7, 0.75)$	$(0.5, 0.6)$
B	$(0.65, 0.66) \times 2$	$(0.3, 0.3)$	$(0.5, 0.75)$	$(0.7, 0.75)$	$(0.3, 0.4)$
Fraction uncertainty $\partial\gamma = 0.025$					

Fig. 14 shows the tracking errors of the case A, which must be compared with Fig. 8. Fig. 14, left, shows the tracking error of the measurements of r_k . At steady state, the tracking error satisfies requirement in Table 1, last row, but because of the uncertainty $\partial\gamma$ bias may become significant as for $6000s < t < 9000s$. Settling time has significantly increased. Fig. 14, right, confirms Theorem 2. Also at steady state, the lower tank tracking error may be biased and more than 50 times larger than requirement. Bias is mainly due to parametric uncertainty.

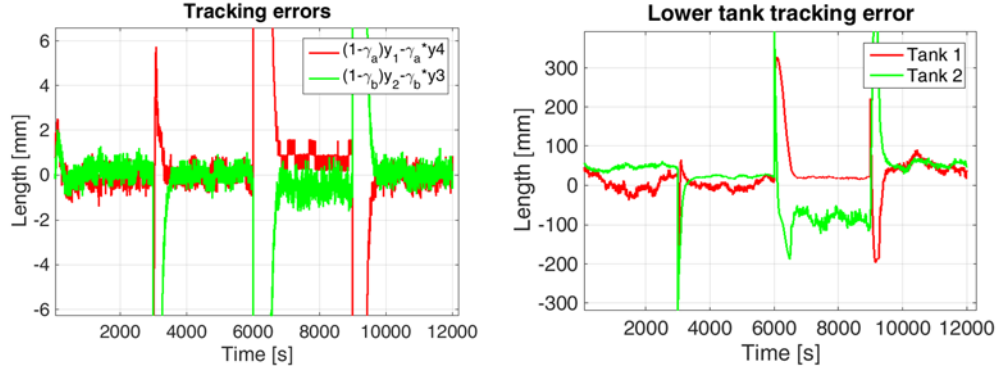


Fig. 14. Case B. Tracking error comparison. Left: controlled levels. Right: tank levels.

Fig. 15 shows the lower tank level trajectory superimposed on the admissible set $A(\gamma)$ defined in Section 2.2. Fig. 15, left, once more confirms Theorem 2, proving the difficulty of Problem B in regulating tank levels. Trajectory in Fig. 15, right, looks wandering more or less than Fig. 15, right, and it stays inside $A(\gamma)$ just because much larger.

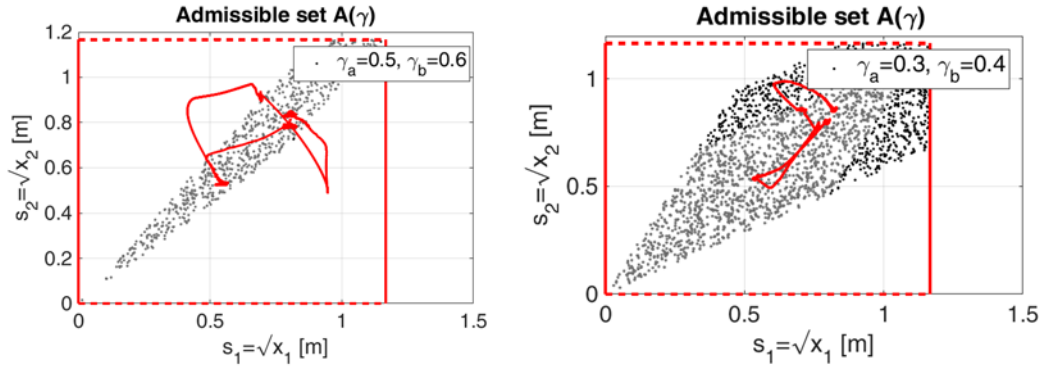


Fig. 15. Lower tank level trajectory for case A (left) and B (right).

Comparison between Problem A and B is in favor of the former both for what concerns simplicity and performance. The only weakness of problem A lays in the limited range of $\beta(\gamma) > 0$. Though from a theoretical standpoint this a significant limitation, it may not be the same in practice. The limitation can be avoided by adopting a direct feedback linearization of the lower tank levels $x_k, k = 1, 2$ as in [16]. Two parallel second order state equations will result as in Problem B, but the output being the lower tank levels to be controlled. Embedded model and disturbance rejection design will be the aim of a future paper.

5. Appendix

We derive equation (29). By assuming $S = S_k$ and by using (2), first and second derivative of the variables in (1) are found to be

$$\begin{aligned}
\dot{r}_1 &= v_1 = (1 - \gamma_a)(-p_1 + p_3) + \gamma_a p_4 + (1 - \gamma_a)\gamma_a(q_{d1} - q_{d4}) \\
\dot{r}_2 &= v_2 = (1 - \gamma_b)(-p_2 + p_4) + \gamma_b p_3 + (1 - \gamma_b)\gamma_b(q_{d2} - q_{d3}) \\
\dot{r}_1 &= \dot{v}_1 = \frac{1-\gamma_a}{2S} \left(\gamma_a \left(\frac{P_4}{\sqrt{x_4}} - \frac{P_1}{\sqrt{x_1}} \right) q_a + (1 - \gamma_b) \frac{P_3}{\sqrt{x_3}} q_b \right) + h_1 + d_1, \\
\dot{r}_2 &= \dot{v}_2 = \frac{1-\gamma_b}{2S} \left(\gamma_b \left(\frac{P_3}{\sqrt{x_3}} - \frac{P_2}{\sqrt{x_2}} \right) q_b + (1 - \gamma_a) \frac{P_4}{\sqrt{x_4}} q_a \right) + h_2 + d_2
\end{aligned} \tag{72}$$

where $\dot{p}_k = \frac{P_k}{2\sqrt{x_k}} \dot{x}_k$, and the nonlinear and disturbance terms hold

$$\begin{aligned}
d_1 &= (1 - \gamma_a)\gamma_a(\dot{q}_{d1} - \dot{q}_{d4}), \quad d_2 = (1 - \gamma_b)\gamma_b(\dot{q}_{d2} - \dot{q}_{d3}) \\
h_1 &= \frac{1-\gamma_a}{2} \left(-\frac{\gamma_a}{1-\gamma_a} P_4^2 - P_3^2 + P_1^2 \left(1 - \frac{P_3 \sqrt{x_3}}{P_1 \sqrt{x_1}} \right) \right) \\
h_2 &= \frac{1-\gamma_b}{2} \left(-\frac{\gamma_b}{1-\gamma_b} P_3^2 - P_4^2 + P_2^2 \left(1 - \frac{P_4 \sqrt{x_4}}{P_2 \sqrt{x_2}} \right) \right)
\end{aligned} \tag{73}$$

Equation (29) and the matrix $B_r(x)$ in (30) follow from (72) upon definition of the components of the sub-matrix $B_{r2}(x)$:

$$\begin{aligned}
B_{r11}(x) &= \frac{1-\gamma_a}{2S} \gamma_a \left(\frac{P_4}{\sqrt{x_4}} - \frac{P_1}{\sqrt{x_1}} \right), \quad B_{r12}(x) = \frac{1-\gamma_a}{2S} (1 - \gamma_b) \frac{P_3}{\sqrt{x_3}} \\
B_{r21}(x) &= \frac{1-\gamma_b}{2S} (1 - \gamma_a) \frac{P_4}{\sqrt{x_4}}, \quad B_{r22}(x) = \frac{1-\gamma_b}{2S} \gamma_b \left(\frac{P_3}{\sqrt{x_3}} - \frac{P_2}{\sqrt{x_2}} \right).
\end{aligned} \tag{74}$$

The determinant of $B_{r2}(x)$ holds

$$\det B_{r2}(x) = \frac{-P_3 P_4}{\gamma_a \gamma_b S_3 S_4} \left(\left(1 - \frac{1}{\gamma_a} \right) \left(1 - \frac{1}{\gamma_b} \right) - \left(1 - \frac{P_1 \sqrt{x_4}}{P_4 \sqrt{x_1}} \right) \left(1 - \frac{P_2 \sqrt{x_3}}{P_3 \sqrt{x_2}} \right) \right), \tag{75}$$

and justifies (31).

6. Conclusions

The paper studies, solves and prove by simulations a pair of control problems for the four-tank benchmark. The aim is to regulate the lower tanks to a sequence of set points within an admissible set, which is dictated by command flow and tank level limits. In the first solution (problem A), the upper tanks are kept unregulated, a way that greatly simplifies model and control algorithms but limits the applicability to the case in which the majority of command flow is dispatched to lower tanks (Theorem 1). To overcome this limitation an alternative solution proposed in the literature (problem B) is investigated and it is shown that is incapable of accommodating unknown disturbance and parametric uncertainty (Theorem 2). Both results are proved by extensive simulation results, and the way to overcome both solution limitations is mentioned. Control algorithms are designed as an exercise of the Embedded Model Control methodology. It allows to accommodate all the uncertainty classes and to reveal design feasibility and how feasibility may be recovered. The reference set of set point sequence can be extended to a generic profile in agreement with tank level and command limitations.

7. Acknowledgments

This work has been partly supported by the National Natural Science Foundation of China (Grant No. 61304041), by the Beijing Higher Education Young Elite Teacher Project (Grant No. YETP0703), and by the Fundamental Research Funds for the Central Universities (Grant No. 2014MS22).

8. References

- [1] K.H. Johansson, "The quadruple-tank process: a multivariable laboratory process with an adjustable zero," *IEEE Trans. Control Syst. Technol.*, Vol.8, No.3, pp. 456-465, May.2000.
- [2] K.H. Johansson, A. Horch, O. Wijk and A. Hansson, "Teaching multivariable control using the quadruple-tank process," *Proc. IEEE Conf. Decision & Control*, Phoenix, Arizona, Vol.1, pp.807-812, December 1999.
- [3] J.B.M. Santos, G. Acioli J, H.C. Barroso and P.R. Barros, "A flexible laboratory-scale quadruple-tank coupled system for control education and research purposes," *Computer Aided Chemical Engineering*, Vol.27, pp. 2151- 2156, 2009.
- [4] E.P. Gatzke, E.S. Meadows, C. Wang, F.J. Doyle III., "Model based control of a four-tank system," *Comput. Chem. Eng.*, Vol.24, No.2, pp.1503-1509, Jul. 2000.
- [5] S. Dadhich and W. Birk, "Analysis and control of an extended quadruple tank process," *Proc. European Control Conf.*, Strasbourg, France, pp.838- 843, 2014.
- [6] P. Husek, "Decentralized PI controller design based on phase margin specifications," *IEEE Trans. Control Syst. Technol.*, Vol.22, No.1, pp.346-351, January 2014.
- [7] N. Arjin, T. Vittaya and T. Thanit, "Design of PID controller for the modified quadruple-tank process using inverted decoupling technique," *Proc. of the 11th Int. Conf. on Control, Automation and Systems*, South Korea, pp.1364-1368, October 2011.
- [8] E.G. Kumar, B. Mithunchakravarthi and N. Dhivya, "Enhancement of PID controller performance for a quadruple tank process with minimum and non-minimum phase behaviors", *Procedia Technology*, Vol.14, pp.480-489, 2014.
- [9] I. Alvarado, D. Limon, D. Muñoz de la Peña, J.M. Maestre, M.A. Ridao, H. Scheu, W. Marquardt, R.R. Negenborn, B. De Schutter, F. Valencia and J. Espinosa, "A comparative analysis of distributed MPC techniques applied to the HD-MPC four-tank benchmark," *J. Process Control*, Vol.21, No.5, pp.800-815, June 2011.
- [10] V. Kirubakaran, T.K. Radhakrishnan and N. Sivakumaran, "Distributed multi-parametric model predictive control design for a quadruple tank process," *Measurement*, Vol.47, pp. 841-854, January 2014.
- [11] S.A. Nirmala, A.B. Veena and D. Manamalli, "Design of model predictive controller for a four-tank process using linear state space model and performance

- study for reference tracking under disturbances,” Proc. of Int. Conf. on Process Automation, Control and Computing, pp.1-5, 2011.
- [12]X. Zhou, C. Li, T. Huang, M. Xiao, “Fast gradient-based distributed optimisation approach for model predictive control and application in four-tank benchmark,” IET Control Theory & Applications, Vol.10, No.9, pp. 1579-1586, 2015.
- [13]H. Gouta, S.H. Said and F. M’sahli, “Model-based predictive and backstepping controllers for a state coupled four-tank system with bounded control inputs: A comparative study,” Journal of the Franklin Institute, August 2015.
- [14]N. Sadati, M. Rahmani and M. Saif, “Two-level robust optimal control of large-scale nonlinear systems,” IEEE System Journal, Vol.9, No.1, pp. 242-251, March 2015.
- [15]J.D. Hedengren et al., “Nonlinear modeling, estimation and predictive control in APMonitor,” Comput. Chem. Eng., Vol.70, pp. 133-148, 2014.
- [16]P.P. Biswas, R. Srivastava, S. Ray and A.N. Samanta, “Sliding mode control of quadruple tank process,” Mechatronics, Vol.19, No.4, pp.548-561, June 2009.
- [17]S. Sutha, P. Lakshmi and S. Sankaranarayanan, “Fractional-order sliding mode controller design for a modified quadruple tank process via multi-level switching,” Computers & Electrical Engineering, Vol.45, pp.10-21, July 2015.
- [18]S.B. Prusty, U.C. Pati and K.K. Mahapatra, “A novel fuzzy based adaptive control of the four tank system,” Proc. of the Third Int. Conference on Computer, Communication, Control and Information Technology, pp.1-6, 2015.
- [19]D. Shneiderman and Z.J. Palmor, “Properties and control of the quadruple-tank process with multivariable dead-times,” Journal of Process Control, Vol.20, No.1, pp.18-28, January 2010.
- [20]A. Numsomran, J. Chaoraingern, T. Trisuwannawat, “The modified quadruple-tanks process: a flexible mathematical model with an adjustable simulink block,” Proc. of the 5th International Conference on Mechanical, Industrial, and Manufacturing Technologies, Penang, Malaysia, March 2014.
- [21]M. Buciakowski, M. de Rozprza-Faygel and J. Ochalek, “Actuator fault diagnosis and fault-tolerant control: Application to the quadruple-tank process,” Proc. of the 11th European Workshop on Advanced Control and Diagnosis, HTW Berlin, Germany, November 2014.
- [22]Y. Alipouri and J. Poshtan, “Optimal controller design using discrete linear model for a four tank benchmark process,” ISA Trans., Vol.52, No.5, pp. 644- 651, September 2013.
- [23]C. Huang and H. Sira-Ramirez, “A flatness based active disturbance rejection controller for the four tank benchmark problem,” Proc. of Amer. Control Conf., pp.4628- 4633, 2015.
- [24]Z. Gao “On the centrality of disturbance rejection in automatic control”, ISA Transactions, Vol. 53, No. 4, July 2014, pp. 850-857.

- [25]E. Canuto, “Embedded model control: outline of the theory,” ISA Transactions, Vol.46, No.3, pp.363-377, June 2007.
- [26]E. Canuto, W. Acuna-Bravo, A. Molano-Jimenez and C. Perez Montenegro, “Embedded model control calls for disturbance modeling and rejection,” ISA Transactions, Vol.51, No.5, pp.584-595, September 2012.
- [27]H. Sira-Ramirez, Z. Gao and E. Canuto, “An active disturbance rejection control approach for decentralized tracking in interconnected systems”, Proc. 13th European Control Conference (ECC 2014), Strasbourg, France, June 24-27, 2014, pp. 588-593
- [28]E. Canuto, L. Colangelo, M. Lotufo and S. Dionisio, “Satellite-to-satellite attitude control of a long-distance spacecraft formation for the next generation gravity mission,” European J. of Control, Vol.25, pp.1-16, September 2015.
- [29]E. Canuto, “On dynamic uncertainty estimators,” Proc. of American Control Conference, pp. 3968-3973, 2015.
- [30]E. Canuto, A. Molano-Jimenez and C. Perez-Montenegro, “Disturbance rejection in space applications: problems and solutions,” Acta Astronautica, Vol.72, pp.121-131, March-April 2012.
- [31]E. Canuto, A. Molano-Jimenez and L. Massotti, “Drag-free control of the GOCE satellite: noise and observer design”, *IEEE Transactions on Control Systems Technology*, Vol. 18, pp. 501-509.
- [32]E. Canuto, D. Carlucci and C. Novara, “Robust stability and control effort minimization by disturbance rejection”, Proc. of 2015 SICE Annual Conference, pp. 666-671, 2015. An extended version has been submitted to *Control Theory and Technology*, 2016.
- [33]E. Canuto, “Drag-free and attitude control for the GOCE satellite,” Automatica, Vol.44, No.7, pp.1766-1780, July 2008.
- [34]E. Canuto, W. Acuna-Bravo, M. Agostani and M. Bonadei, “Digital current regulator for proportional electro-hydraulic valves featuring unknown disturbance rejection”, *ISA Transactions*, Vol. 53 No. 4, pp. 909-919, 2014.
- [35]A. A. Prasov and H. K. Khalil “A nonlinear high-gain observer with measurement noise in a feedback control framework”, *IEEE Trans. Autom. Control*, vol. 58, No.3 March 2013, pp.569-580.
- [36]C. Mohtadi “Bode’s integral theorem for discrete-time systems”, IEE Proceedings, Part D, Vol. 137, No. 1999, pp. 57-66.